Nanoscale Advances

ROYAL SOCIETY OF CHEMISTRY

REVIEW

View Article Online
View Journal | View Issue

Cite this: *Nanoscale Adv.*, 2023, **5**, 6318

A review of metal–organic framework (MOF) materials as an effective photocatalyst for degradation of organic pollutants

M. Shahnawaz Khan, [a] Yixiang Li,[a] Dong-Sheng Li, [b] Jianbei Qiu,[c] Xuhui Xu [c] and Hui Ying Yang *[a]

Received 10th August 2023
Accepted 30th September 2023

DOI: 10.1039/d3na00627a

rsc.li/nanoscale-advances

Water plays a vital role in all aspects of life. Recently, water pollution has increased exponentially due to various organic and inorganic pollutants. Organic pollutants are hard to degrade; therefore, cost-effective and sustainable approaches are needed to degrade these pollutants. Organic dyes are the major source of organic pollutants from coloring industries. The photoactive metal–organic frameworks (MOFs) offer an ultimate strategy for constructing photocatalysts to degrade pollutants present in wastewater. Therefore, tuning the metal ions/clusters and organic ligands for the better photocatalytic activity of MOFs is a tremendous approach for wastewater treatment. This review comprehensively reports various MOFs and their composites, especially POM-based MOF composites, for the enhanced photocatalytic degradation of organic pollutants in the aqueous phase. A brief discussion on various theoretical aspects such as density functional theory (DFT) and machine learning (ML) related to MOF and MOF composite-based photocatalysts has been presented. Thus, this article may eventually pave the way for applying different structural features to modulate novel porous materials for enhanced photodegradation properties toward organic pollutants.

1. Introduction

Environmental pollution resulting from population growth and industrialization has led to water scarcity, posing a significant challenge for human beings.[1,2] Moreover, this challenge has been exacerbated by unpredictable climate change and the impending global warming crisis.[3] In response to the freshwater crisis, water purification has emerged as an alternative drinking and industrial water supplementation solution.[4,5] Therefore, developing efficient technologies that effectively remove contaminants from wastewater becomes crucial, ensuring environmental stability.[6,7] Based on the Safe Drinking Water Act (SDWA), contaminants can be categorized as organic and inorganic, depending on their chemical composition.[8] Inorganic pollutants encompass a range of cations, oxo-anions, and heavy metal ions, including radioactive elements, which are of utmost ecological concern.[9,10] On the other hand, organic pollutants constitute a diverse group that includes pharmaceuticals and personal care products (PPCPs), dyes, oils, polyaromatic hydrocarbons, detergents, pesticides, insecticides, and herbicides.[11,12] Although their concentrations may not be as high as those of their inorganic counterparts, organic pollutants are particularly concerning due to their high stability and long-term environmental impact. Wastewater treatment plants cannot effectively eliminate these pollutants and they may persist for extended periods, possibly degrading into more toxic byproducts.[13] The field of organic pollutant degradation encompasses various technologies (Fig. 1); however, traditional methods like coagulation/flocculation precipitation, biological, adsorption, and membrane technology have limitations such as high operational costs, generation of secondary pollutants, and low efficiency.[14–18] In contrast, advanced oxidation processes (AOPs), particularly photocatalytic AOPs, have gained significant consideration due to their simplicity, environmental friendliness, and sustainability.[19] Through photocatalytic AOPs, organic pollutants can be disintegrated into less toxic compounds.[20]

While photocatalytic processes harness the energy of light to generate reactive oxygen species (ROS) that can oxidize organic pollutants, the kinetics of these reactions can be influenced by factors such as catalyst stability, recombination of charge carriers, and the availability of target pollutants at the catalyst surface.[21–23] Therefore, we must consider the underlying mechanisms involved in photocatalytic performance. Mechanistically, photocatalytic processes involve the excitation of e^- from the valence band (VB) to the conduction band (CB) of the

[a]*Pillar of Engineering Product Development, Singapore University of Technology and Design, 8 Somapah Road, 487372, Singapore. E-mail: yanghuiying@sutd.edu.sg*

[b]*College of Materials and Chemical Engineering, Key Laboratory of Inorganic Nonmetallic Crystalline and Energy Conversion Materials, China Three Gorges University, Yichang, 443002, P. R. China*

[c]*Key Laboratory of Advanced Materials of Yunnan Province, Kunming University of Science and Technology, Kunming, Yunnan 650093, China*

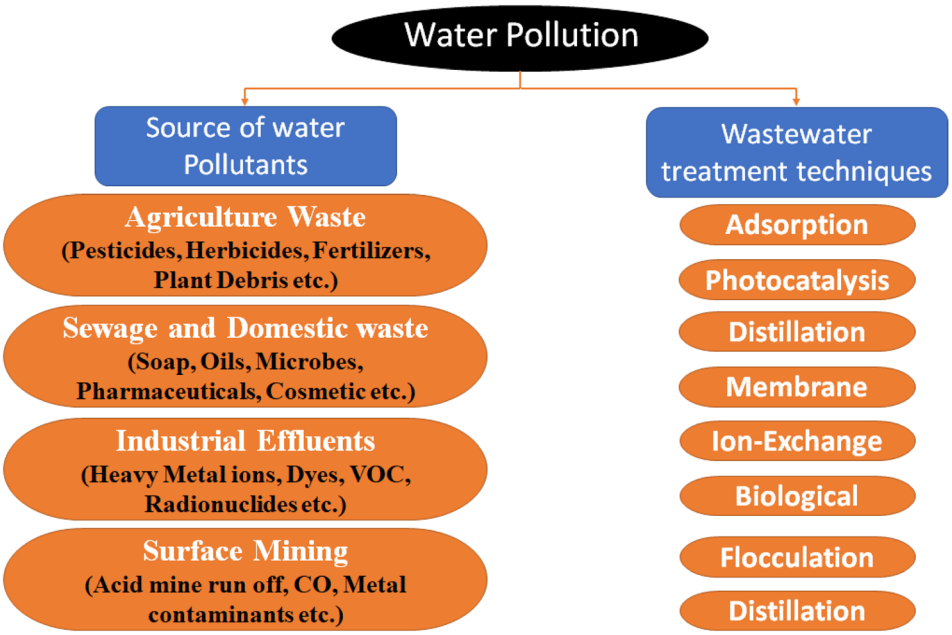

Fig. 1 Different sources and treatment techniques of wastewater.

photocatalyst material upon absorption of light leading to the formation of e^{-}–h^{+} pairs.[24,25] Subsequently, these charge carriers can participate in redox reactions with adsorbed organic molecules or water, generating ROS like hydroxyl radicals ($^{\bullet}OH$) and superoxide radicals ($^{\bullet}O^{2-}$) which are mostly responsible for degradation of organic pollutants into less harmful inorganic ions. The rate of these reactions is highly dependent on the availability of these charge carriers and their spatial separation to minimize recombination.[26]

Hence, there is a need to develop novel materials that can facilitate abundant light absorption, high stability and enhance photocatalytic performance.[27] Metal–organic frameworks (MOFs), composed of metal nodes and organic ligands, possess crystalline structures due to their high porosity, diverse topology, and customizable physicochemical properties; they dispense several applications.[28–31] In recent decades, MOFs have demonstrated great potential in photocatalytic degradation of organic pollutants. MOFs such as MOF-5 ($Zn_4O(BDC)_3$, where BDC represents 1,4-benzene dicarboxylate), MIL-125 ($Ti_8O_8(OH)_4(BDC)_6$), and UiO-66 ($Zr_6O_4(OH)_4(BDC)_6$) exhibit semiconductor-like behavior.[32] MOFs having metal ions and organic ligands, acting as separated semiconductor quantum dots with light-absorbing antennas.[22,33,34] Therefore by these results, researchers have developed various light-responsive MOFs for organic pollutant degradation, CO_2 fixation, hydrogen production, selective organic transformation, and bacterial disinfection in wastewater.[35] On the other side of the story, a green material, polyoxometalates (POMs), also exhibits unusual photocatalytic activity in removing organic pollutants from wastewater.[36]

POMs possess stable structures, redox properties, multiple catalytic sites, and high stability during photocatalytic processes.[37] But they have weakly visible light absorbance, and their photoexcitation requires irradiation with only UV light; thus, their light utilization property is very poor. Recent studies indicate that compositing POMs with MOFs can yield stable and efficient hybrid photocatalysts. This combination offers several advantages: (i) POMs exhibit brilliant photosensitivity comparable to semiconductors like TiO_2; (ii) the integration of POMs with MOFs enhances material stability in aqueous environments, enabling reusability and reducing the generation of secondary pollutants; (iii) POM-based MOFs provide a versatile platform for designing various hybrid structures and activating catalysts for the degradation of organic dyes.[38–42] Hence, this review aims to explore the current literature on MOFs and POM-based MOF composite photocatalysts for the degradation of organic pollutants under UV and visible light. Lastly, several theoretical analysis approaches such as machine learning (ML) and Kohn–Sham DFT have also been discussed in detail for achieving ultimate photocatalysis performance.

2. Metal organic frameworks (MOFs)

2.1 Fundamentals of metal–organic frameworks (MOFs)

Metal–organic frameworks (MOFs) are a class of porous materials constructed by metal nodes/clusters and organic linkers, forming numerous architectures.[43–46] The metal ions can create compounds with unique coordination modes, having tetrahedral, trigonal bipyramidal, square planar, and octahedral geometries.[47] Meanwhile, the most used organic linkers are polytopic carboxylates and other aromatic heterocyclic molecules, facilitating coordination chemistry with the metal ions.[48] The solvothermal method is the most widely accepted technique for designing MOFs. However, alternative techniques such as slow evaporation, mechanochemical, ultrasonic, layering, microwave-assisted, and electrochemical methods have

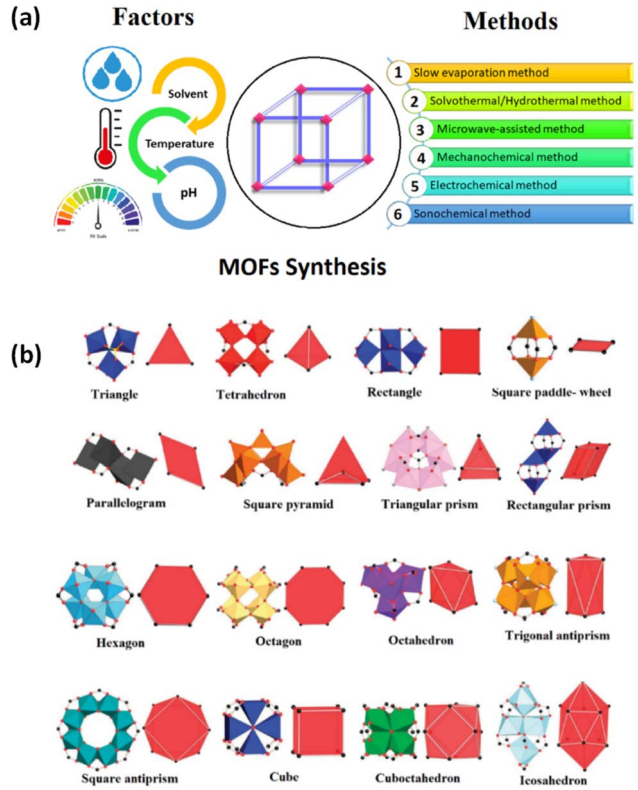

Fig. 2 (a) Overview of synthesis strategies of MOFs; (b) examples of some secondary building units (SBUs) in MOFs.[9] This figure has been adapted from ref. 9 with permission from Elsevier, copyright 2023.

also been employed (Fig. 2a).[1,9,49] The versatility of MOFs has led to their applications in diverse fields, spanning from materials and chemicals to biological sciences.[50–60] While certain metal ions, such as Co(II), Cd(II), Eu(III), and Ag(I), may be toxic or expensive, they are still employed to gain insights into the fundamental of metal–organic chemistry.[61] Over time, significant progress has been made, but certain limitations need to be addressed before MOFs can be commercialized for industrial use.[62–64] Additionally, there have been reports of water-stable and light-responsive MOFs capable of removing organic pollutants from wastewater.[65] The wide variety of organic linkers and metal ions in MOFs allows tuning them to form secondary building units (SBUs) for target-specific pollutants using solar energy (Fig. 2b).

In some cases the investigation also focused on degrading dyes using photoactive MOFs under light irradiation, with the assistance of H_2O_2 as an oxidant.[66] Initially, the catalytic activity of traditional MOFs like MOF-5, MIL-125, and UiO-66, which exhibit semiconductor-like behavior, has been explored.[32] Ye *et al.* compared the catalytic activity of MIL-101(Fe), MOF-5, MIL-125(Ti), and UiO-66(Zr) with traditional semiconductors, particularly in dye degradation, and found that these MOF composites exhibited better photocatalytic performance.[67] Qiu *et al.* reviewed various methodologies for tuning photocatalysts to enhance their performance.[68] On the other hand, Bedia *et al.* reported the methodologies and characterization of MOF-based catalysts for water treatment, while another report focused on Fe-based MOFs for visible light degradation of various pollutants.[69,70] Ma and co-workers also discussed several strategies to improve the photocatalytic performance of pristine MOFs, such as mixed linker or metal strategies, linker functionality, dye sensitization, and linking of metal nanoparticles.[33,71–73] Similarly, Mohammad *et al.* described various strategies to enhance the photocatalytic performance of MOF materials in solar light with surface modification and interfacial construction techniques.[74] Other reports also discussed MOF-based materials with enhanced photocatalysis performance for wastewater treatment.[75–77]

2.2 Environmental applications of MOFs

Environmental pollution has emerged as a significant crisis in the 21st century, primarily driven by the increasing global population and industrialization.[78–80] One of the critical challenges faced by the world is the scarcity of drinkable water, particularly in developing nations.[81,82] Water pollution refers to any contamination that alters the chemical and physical properties of water.[57,80,82,83] Water pollution caused by numerous pollutants, including antibiotics, phthalates, heavy metals, pesticides, and polyaromatic hydrocarbons (PAH), poses a significant threat to the environment and human health.[56,78] These known pollutants can adversely affect ecological and human well-being, yet their behavior and ecotoxicological impacts are often overlooked.[84] They can originate from various sources, such as pesticides and herbicides used in agriculture, manufacturing additives like plasticizers and gasoline, pharmaceutical drugs found in municipal and livestock wastewater, personal care products such as insect repellents, fragrances, sunscreen agents, microbeads, and disinfectants commonly found in municipal waste.[85,86] On the other hand, organic dyes, commonly found in effluents from industries such as rubber, plastics, leather, cosmetics, and textiles, pose significant environmental and health risks due to their carcinogenic nature and resistance to degradation by biological processes.[87,88] A substantial number of dyestuffs, approximately 7×10^5 tons, is used globally in industries, and around 10% of this amount is lost as industrial effluents in water bodies. These dyes are stable in water and pose challenges for conventional treatment methods.[89] Techniques like liquid chromatography–tandem mass spectrometry have been employed to detect trace amounts of these contaminants in wastewater, highlighting the need for prioritizing water policy and disposal control.[35,85,86,90] While certain materials used for purification may have low effectiveness, high cost, and the potential to generate additional pollutants, MOF materials offer a promising solution to address these challenges. However, common issues associated with MOFs include structural integrity and metal leaching. Furthermore, the functional property and stability of MOFs heavily rely on the synergic interaction between metal nodes and organic ligands. Fine-tuning the MOFs makes it possible to enhance their photodegradation properties.

MOFs are used in environmental applications, specifically focusing on the photodegradation of organic dyes.[91] The first report on the adsorption of methyl orange (MO) by a MOF was

published in 2010, while the photocatalytic performance for phenol degradation was documented in 2007.[92–95] The photodegradation process has a certain edge compared to the adsorption process due to its high efficiency and complete degradation of the target product. MOF-based composites, specifically POM-based MOFs, have shown potential in degrading organic dyes,[96] specifically, the Keggin-type cluster within POM-based catalysts, but their design and structure–activity relationship have not been extensively investigated.[97] Moreover, using simple POM based photocatalysts is difficult due to their lower stability and difficulty in absorbing light. Therefore, POM-based MOFs offer multiple catalytic centers and tunable light-absorbing areas, enhancing their photocatalytic performance.[98] This review article explores the existing literature on pristine MOFs and MOF-based composites, with a particular focus on MOFs containing POMs, and how they improve photocatalytic performance.

2.3 Shortcomings of MOFs

MOF-based materials demonstrate exceptional efficiency attributed to their high porosity, surface area, and customizable architecture.[99,100] However, the stability of MOFs has consistently been a concern when employing in wastewater treatment applications (Fig. 3).[101]

The low intrinsic stability of MOFs stems from the weak bonding between metal ions and organic ligands. Moreover, the stability of MOFs can exhibit variations depending on factors such as pH conditions, humidity, and temperature.[102] However,

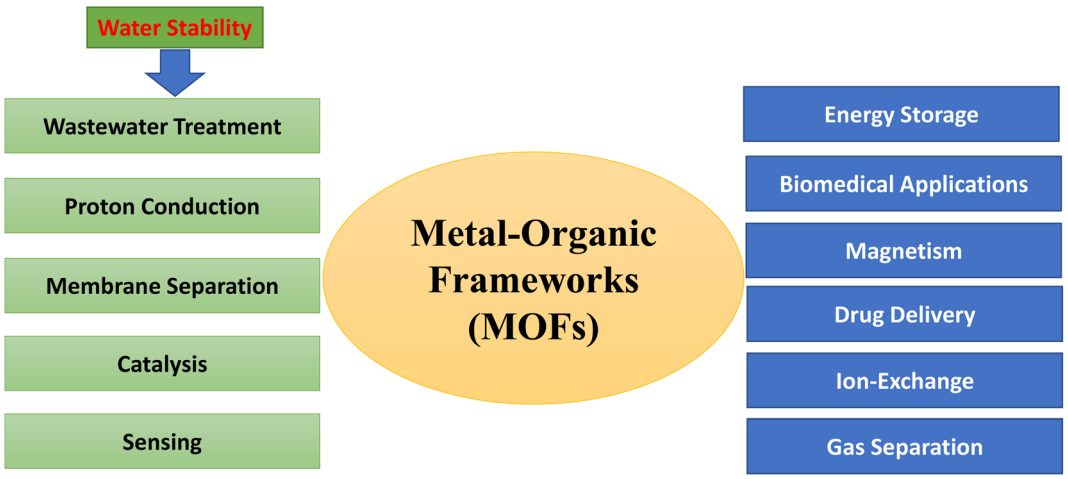

Fig. 3 Various applications of pristine MOFs and water-stable MOFs.[1,9,62]

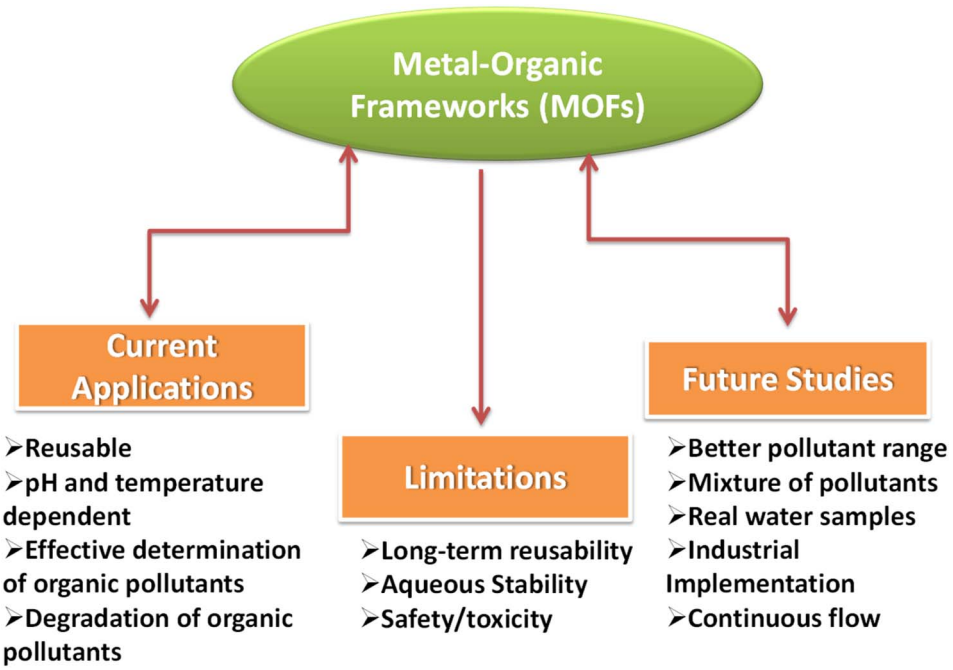

Fig. 4 Current and future trends in MOFs.

their stability can be easily tuned by changing the metal ion, organic linkers, or the oxidation state of the metal ions.[103,104] Post-synthetic modifications (PSM) of MOFs also offer intriguing possibilities for designing water-stable MOFs.[105] While many water-stable MOFs and their composites have demonstrated excellent activity, some are composed of toxic metal ions like Cr, Cd, and Ag, along with potentially harmful organic linkers.[90] For MOFs, it is important to consider the potential release of toxic elements during the degradation of MOFs.[106] In practical applications, certain materials, such as tap water or real water samples, may exhibit poor performance under real conditions.[107] Another challenge with MOFs in water treatment is the leaching of MOFs or ligands.[108,109] Additionally, the recyclability of MOFs is an important aspect, as some materials lack reusability in water treatment processes.[110] Furthermore, the photocatalytic activity of MOF materials presents challenges, including narrow band gaps, various additives such as H_2O_2 and sulfate species, and the generation of toxic byproducts during the catalytic process.[111] These factors need to be addressed to optimize the photocatalytic performance of MOFs and ensure their effectiveness in treating water pollutants.[112] Fig. 4 illustrates the various applications, current studies, and prospects of MOF-based materials.

3. Removal of organic pollutants by MOFs and their composites

3.1 Principles of photocatalytic degradation

Persistent Toxic Substances (PTS), which encompass a group of toxic chemicals that persist in the environment, bioaccumulate in organisms, and pose significant risks to human health and the environment (Table 1), include organic dyes as one example.[113] Due to their complicated structure, organic dyes are known to be particularly challenging to degrade.[114]

Several processes can be involved to remove aromatic dyes, such as chemical, biological, electrochemical, and ion exchange.[115,116] The biological method utilizes microorganisms and is environmentally friendly but requires suitable external conditions.[117] Chemical methods can be inefficient due to their high operational costs, while physical methods offer potential solutions but may not be widely adopted in conventional water treatment.[117] Therefore, various other technologies have been developed to address these issues, such as carbon treatment, heterogeneous catalysis, chlorination, and biodegradation.[118] Among these technologies, advanced oxidation processes (AOPs) have attracted tremendous interest due to their ability to remove contaminants from wastewater by photocatalytic processes.[119–121] The photocatalytic process involves catalysts to produce highly reactive free radicals, such as $^{\bullet}OH$ and $^{\bullet}O_2^-$ in the presence of light, which can efficiently degrade organic dyes into inorganic ions, resulting in water purification.[25,122] Investigating the intricate mechanisms governing MOF materials' performance in photocatalysis reveals a multifaceted interplay of interactions. Notably, adsorption stands as the initial interaction within the photocatalytic process, necessitating a comprehensive understanding of this mechanism.[123] This mechanism encompasses several pivotal interactions between MOFs and organic pollutants, including electrostatic interactions, π–π interactions, acid–base interactions, and hydrophobic interactions, among others (Fig. 5). It's noteworthy that instances occur where a combination of these interactions influences the adsorption of organic pollutants.[124] Electrostatic interactions assume a pivotal role in the removal of hazardous substances from aqueous environments.[125] The surface charge of the MOF undergoes modulation when exposed to polar media like water. These surface charge alterations are contingent upon the water's pH. Furthermore, charged MOFs readily engage with oppositely charged adsorbates, constituting electrostatic interactions.[126] Another crucial mechanism governing MOF–organic pollutant interactions is hydrogen bonding. This interaction typically occurs when the MOF material possesses accessible functional groups capable of forming hydrogen bonds with organic pollutants.[127] π–π stacking represents another prevalent mechanism in various adsorption processes, particularly with aromatic compounds or adenine over MOF materials. π–π interactions occur between organic ligands and organic pollutants, augmenting MOFs' removal efficiency.[128]

Table 1 Classification, sources, and hazards of persistent toxic substances (PTS)[1]

PTS	Sources	Hazards
Synthetic dye	The food industry, dye wastewater, papermaking wastewater, textiles, and printing wastewater	High chromaticity, carcinogenesis, toxicity
Plasticizer	Chemical industry and plastics industry	Inhibition of the human central nervous system, strong stability
Polycyclic aromatic hydrocarbon (PAH)	Petrochemical industry and coking industry	Strong stability, strong carcinogenicity
Organic cyanogen compounds	Petrochemical industry, artificial fibre industry, coking industry	Acute toxicity
Heterocyclic organisms	Heterocyclic organisms	Carcinogenesis, strong stability mutagenicity, bioconcentration
Polychlorinated biphenyl (PCB)	The lubricating oil industry, chemical wastewater, mechanical industry, plastics industry	Acute toxicity, carcinogenesis
Synthetic detergent	The food industry, textile industry, tannery industry, papermaking industry	Solubilization for carcinogenic polycyclic aromatic hydrocarbons

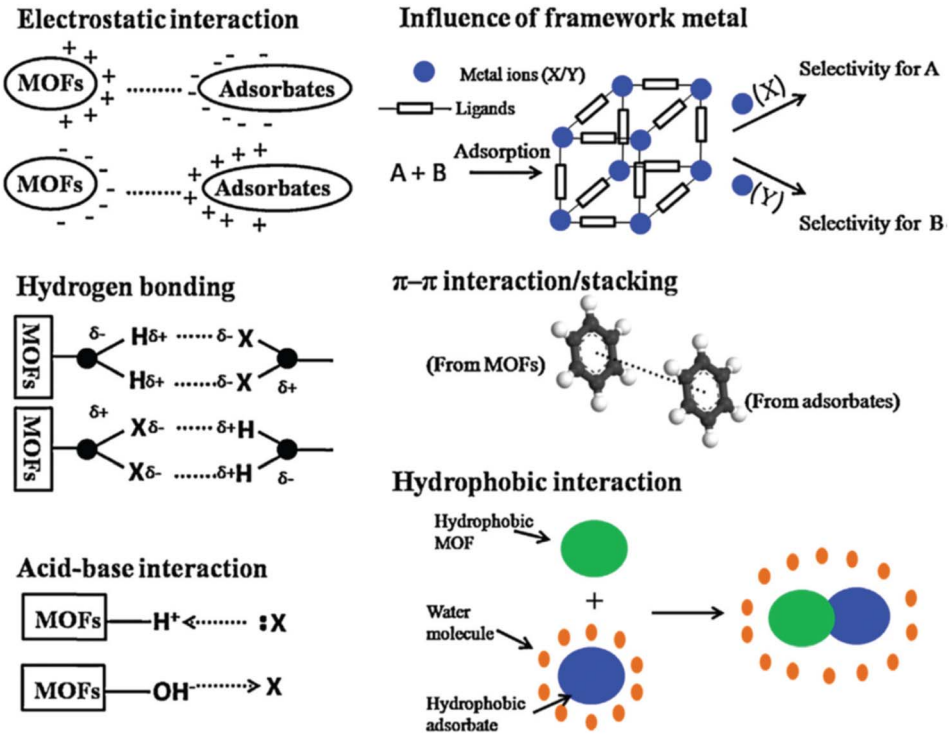

Fig. 5 Schematic diagram of the possible mechanisms for the adsorptive removal of hazardous materials over MOFs.[123] This figure has been adapted from ref. 123 with permission from Elsevier, copyright 2015.

While not as commonplace, acid–base interactions can also play a significant role in organic pollutant removal using MOF-based materials. In such cases, MOFs are functionalized with acid or base groups to interact with organic pollutants in water. It's worth noting that pristine MOFs may not exhibit optimal adsorption performance, but functionalized MOFs with acid or base groups often display superior removal capabilities.[129] Hydrophobic interactions are frequently observed during the adsorption of organic compounds from aqueous solutions. Hydrophobic substances, characterized by their nonpolar nature, low water solubility, and extended carbon chains, are predisposed to engage in such interactions. MOFs have found utility in applications related to the adsorption of spilled oil, although this application is not as widespread.[130]

Thus, TiO_2 gained significant attention initially due to its chemical and biological inertness, cost-effectiveness, strong oxidizing power, and non-toxic nature. However, TiO_2 has a wide bandgap energy of 3.2 eV, limiting its absorption to only UV light.[131] Consequently, researchers have explored various metal oxides and sulfides, such as CoS_2, In_2S_3, CdS, and Sb_2S_3, exhibiting effective catalytic activity in visible light by properly manipulating their conduction band (CB) and valence band (VB). However, these traditional semiconductors suffer from photo corrosion, generating secondary pollutants like heavy metal ions.[132] Therefore, researchers need to develop novel materials with higher efficiencies and better utilization of solar light for degrading organic pollutants largely offered by MOF and its composite materials (Table 2). Like other

Table 2 The advantages and disadvantages of different dye removal technologies[1]

Technology	Disadvantages	Advantages
Photochemical process	The formation of by-products and power consumption	No sludge production, rapid, high efficiency, simple operation
Membrane separation	Short lifetime, economically unfeasible	High efficiency, reuse salts
Electrochemical process	High electricity consumption and economically unfeasible	High efficiency, rapid
Ion change	Economically unattractive, ineffective to certain dyes	No loss of sorbents
Coagulation/flocculation	High sludge production and disposal issues	Simple, economically attractive
Adsorption	Ineffective to certain dyes, the regeneration is costly, exposing adsorbent residue is also an issue, as loss of adsorbents	Low cost, won't form hazardous substances
Biodegradation	Occupy a certain land area, require strict external environmental conditions, and slow process	Economically attractive and simple

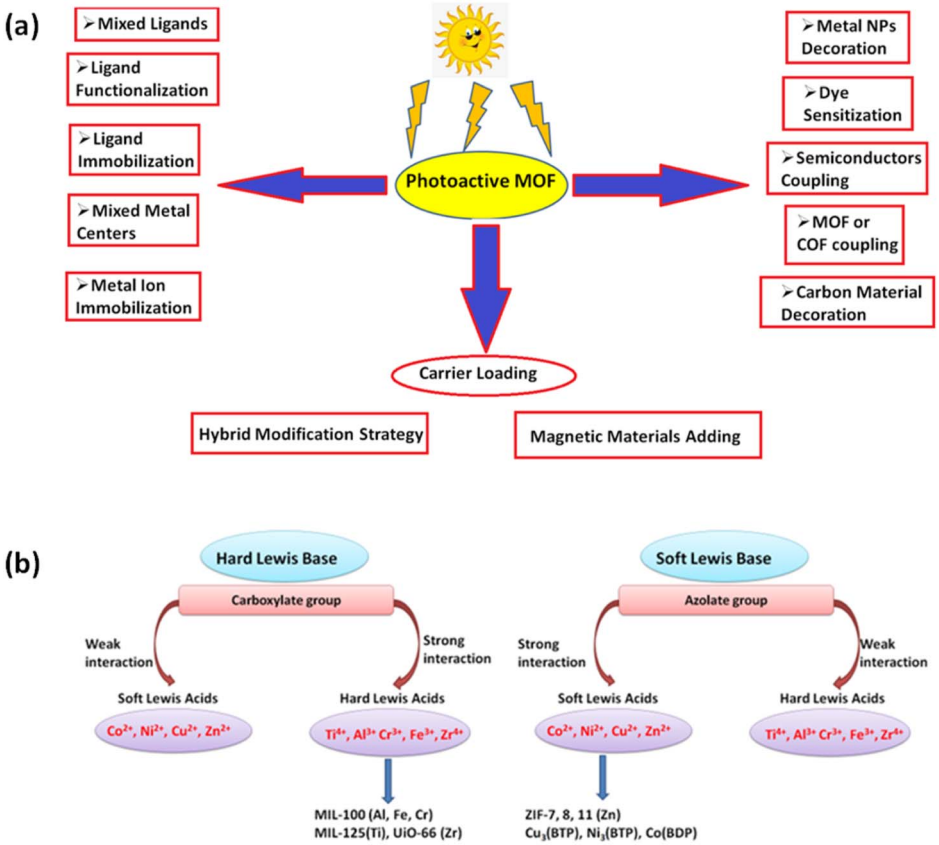

Fig. 6 (a) Strategies to engineer MOFs as efficient photocatalysts for environmental applications; (b) strategies to construct stable MOFs by carboxylate and azolate groups guided by HSAB theory.

semiconductors, MOFs possess CB and VB attributed to the empty outer metal and organic ligand orbitals.[133] While MOFs can have diverse functionalized ligands and metal ions in their structures, PSM is often required to introduce functional groups such as metal oxides, organic dyes, amines, and quantum dots.[134] On the other hand, superior light-absorbing capacity compared to traditional photocatalysts is also a key feature of such materials. Furthermore, the well-defined crystalline structure of MOFs facilitates their characterization and enables the assessment of the relationship between their topology and photocatalytic performance (Fig. 6a). It is important to note that comparing the photocatalytic performance of MOFs to traditional semiconductors is not feasible due to the former's lower solar energy conversion and charge separation efficiency. However, incorporating various functional materials into MOFs can overcome these limitations.[133]

Before we explore the latest research on MOF-based photocatalysts, let's first talk about an important idea called 'band gap engineering,' which helps us use visible light effectively in photocatalytic reactions. Band gap engineering is also a fundamental concept focused on adjusting the energy band gap towards lower values by carefully controlling the crystal structure of MOFs. This concept is particularly significant in the realm of photocatalysis, where narrowing the band gap energy is essential to enable efficient photocatalytic activity within the visible or near-infrared spectrum.[135] Recent literature has introduced several molecular strategies aimed at optimizing and reducing the band gap energy of these materials.[136] It is widely recognized that band gap engineering primarily hinges on two key components: the organic linker and the metal ions within the MOF structure. Researchers, such as Volkmer *et al.*, have proposed several strategies for reducing the band gap energy: (i) increasing the level of conjugation in the organic linkers can raise the valence band (VB) energy, resulting in improved absorption in the visible spectrum. (ii) The choice of metal ions with partially unoccupied d-orbitals can effectively lower the conduction band (CB) energy level, facilitating efficient electron transfer processes. (iii) Introducing electron-rich fragments strategically into the MOF nodes has been explored to modify the electronic properties and thus the band gap energy.[137]

Additionally, Allendrof *et al.* have suggested the same approaches to engineering the electronic properties of MOFs, including altering the metal ions, modifying organic linkers, and incorporating selected organic fragments into the MOF frameworks.[138] Conversely, Syzgantseva *et al.* have investigated the correlation between the electronic parameters of MOF components and their band structures, utilizing factors like ionization potential and electronic affinity of organic linkers and metal oxides to assess the alignment of metal states and the energy positions of organic linker states within MOFs.[139]

Ultimately, the ability to tune the band gap energy in MOFs is typically achieved through adjustments to linkers or variations in metal nodes, both of which are widely accepted strategies. For MOFs with limited light-harvesting capabilities, tuning linkers and incorporating other metals *via* doping can be particularly effective in reducing band gaps. Moreover, the long-term application of MOFs in photocatalytic organic pollutant degradation necessitates attention to their thermal and chemical stability. In this regard, tuning the band gap of MOFs, in conjunction with principles such as the hard–soft acid–base (HSAB) concept, can be instrumental in enhancing the stability of MOF materials. This comprehensive approach to band gap engineering not only improves our understanding of MOF-based photocatalysts but also offers valuable insights for their practical application in environmental remediation and sustainable energy generation.

3.2 Photocatalytic degradation of organic pollutants by MOFs

Recently, there has been a growing trend in utilizing MOFs that can be easily transformed into nano-sized inorganic semiconductors for degrading organic pollutants under UV or visible light. In this regard, Wang and coworkers have contributed significantly by reporting several composites derived from MOFs for photocatalysis. These composites include Bi_2MoO_6, ZIF-67, Fe_3O_4@MIL-100(Fe), α-$Bi_2Mo_3O_{12}$, $[Cd(dcbpyno)(bix)_{1.5}]\cdot 2H_2O$/PANI, and Pd@UiO-66($NH_2$), all of which exhibit enhanced photocatalytic activity.[133,140] Flexible MOFs as semiconductor materials in artificial photosynthesis can enhance the reaction template for light harvesting and catalytic sites.[141] By improving organic ligands, the absorption of light bands can be accommodated through electron localization, the transition from metal–ligand cluster charge transfer, $\pi \rightarrow \pi^*$ transition, and ligand $\rightarrow$ metal cluster charge transition in the conjugated ring, ultimately advancing the photocatalytic activity of MOFs. Mobile charge carriers activate the metal clusters, facilitating heterogeneous photo–redox reactions.[142] The first-ever MOF studies by Zecchina's group confirmed the optical and vibrational qualities of MOF-5 using DRS, luminescence, and Raman analysis. It was discovered that the SBU of MOF Zn_4O_{13} could act as quantum dots and a light-absorbing antenna.[143] After that, Garcia's research group demonstrated the semiconductor properties of MOF-5 through laser flash photolysis. The photocatalytic activity of MOF-5 was utilized to disintegrate phenol, and the charge transfer movement of MOF-5 was observed through photoluminescence spectra.[144] Followed by the MIL and UiO series, recognized as the two most prestigious MOF series, known for their exceptional stability and dispense high photocatalytic performance.[145] These series primarily involve first transition metal ions such as Co^{2+}, Ni^{2+}, Cu^{2+}, and Zn^{2+}, which can interact with lewis bases like azolate to create robust MOFs (Fig. 6b).

UiO-66 (Zr) exhibits remarkable photocatalytic capability for hydrogen evolution due to its extra water stability.[146] On the other hand, developing efficient photocatalytic by modifying NH_2-MIL-125(Ti) by introducing an amino-functionalized linker (H_2ATA).[147] The addition of the $-NH_2$ group in the organic ligand did not significantly impact the structural stability of MIL-125(Ti) but greatly enhanced its photocatalytic performance, optical absorption, and CO_2 adsorption capacity. Notably, MIL series such as MIL-88B(Fe), MIL-101(Fe), and MIL-53(Fe) can be employed in aqueous suspensions to activate persulfate, generating $^{\bullet}SO_4^-$ and $^{\bullet}OH$ species that effectively decompose Acid Orange-7 (AO-7).[148] Subsequently, MIL-101(Fe) was utilized for the degradation process, exhibiting the highest degradation efficiency of approximately 93.1% within a 4 h.[149] The study reveals that the degradation of AO-7 using MIL-88B(Fe) was insignificant. However, other researchers have extensively investigated the 100% degradation of MB in 3.5 h using MIL-88B(Fe) by introducing H_2O_2 and light. These findings validate that incorporating appropriate substances and targeted degradation pollutants can enhance photocatalytic performance. Another research on MIL-53 demonstrates remarkable thermal stability within the MIL series, with MIL-53(Fe) and MIL-53(Al) notable examples.[150] These results inspired Chatterjee *et al.* to synthesize a binary MOF known as MIL-53(Al–Fe)@SiO_2.[151] The integrated MOF with pulverized coal aluminum foil and $FeCl_3$ ensures photosensitivity and non-toxicity. It was observed that under visible light, and initial concentrations of 10 and 30 ppm, the photodegradation rates of MIL-53(Al–Fe)@SiO_2 were 89.34% and 54.87%, respectively. Conversely, no appreciable photocatalytic activity was observed when the monomeric unit of the metal salt was used. Furthermore, the photocatalytic activities towards MB were examined, yielding 99.95% and 94.06% degradation rates to MIL-53(Al–Fe)@SiO_2 and 72.42% and 67% for MIL-53(Al)@SiO_2 under 8 W UV light. Comparing the performance of these two materials revealed that Al, Fe, and SiO_2 impede the recombination of electrons and holes, effectively reducing the band gap. Consequently, the mechanism can be explained by the ability of acidic material to absorb more water molecules, generating an increased amount of hydroxyl groups, thereby enhancing the photocatalytic activity. Notwithstanding, the initial step in the photocatalytic experiment involves adsorption, which directly affects the degradation efficiency. In many instances, MOFs can photo-catalytically degrade dyes and absorb UV light, limiting solar energy utilization. Therefore, combining MOF with semiconductor materials and photosensitive initiators for environmental preservation using solar light requires sensible consideration.[152] Araya and their colleagues successfully enhanced the degradation of SRB by employing MIL-53(Fe) with cationic resin.[153] The research findings revealed the significant contribution of the adsorption process to the photocatalytic performance of the MOF. Hence, MOFs based composites must enhance the photosensitivity and light absorption capabilities.[154] Conversely, pristine MOFs have seen limited utilization in degrading organic pollutants, while nano-sized MOF materials and POM-based MOF materials have gained prominence due to their numerous active sites and functional behavior.[155,156] In a recent report, Kim *et al.* conducted a study that synthesized a Zr-based MOF using pyrene and porphyrin building blocks, resulting in a nano-sized material.[157] The nano size mixed ligand MOF (nMLM) was employed to degrade Rh-B in the

presence of H_2O_2. The nanoscale MOF (n-MOF), with its various catalytic active sites, demonstrated remarkable efficiency and completely degraded the Rh-B within 240 min (Fig. 7a). The efficiency of the n-MOF is more than that of nanoscale PCN-222 (n-PCN-222) and nanoscale NU-1000 (n-NU-1000) (Fig. 7b). The enhanced performance of nMLM is due to the enhanced light harvesting capability of porphyrin ring which triggers the energy transfer from the pyrene ring and prevents the e^-–h^+ recombination. The findings suggest that the energy transfer between the pyrene and porphyrin ring improved the light-harvesting ability. The calculated rate constant was determined in the case of nMLM, was 0.01117 min^{-1} higher than that of n-NU-1000 and n-PCN-222 (Fig. 7c). Also, the nMLM dispenses the better recyclability test up to three photocatalytic cycles (Fig. 7d). The mechanism behind such fantastic photocatalytic performance of nMLM is due to the photogenerated hole in the reaction. Based on the literature, the author describes the absorption of light pyrene in the nMLM acts as an antenna and receives energy to be transferred to the porphyrin ring. Subsequently, porphyrin becomes photoexcited, and some e^- have been transferred to the Zr-oxo cluster, generating the $^{\bullet}O_2^-$. Henceforth, the e^- and h^+ are separated, preventing rapid recombination within the porphyrin ring. Thus, nMLM causes energy transfer to porphyrin due to the synergistic effect of pyrene and porphyrin, leading to the effective charge separation in the ring (Fig. 7e).

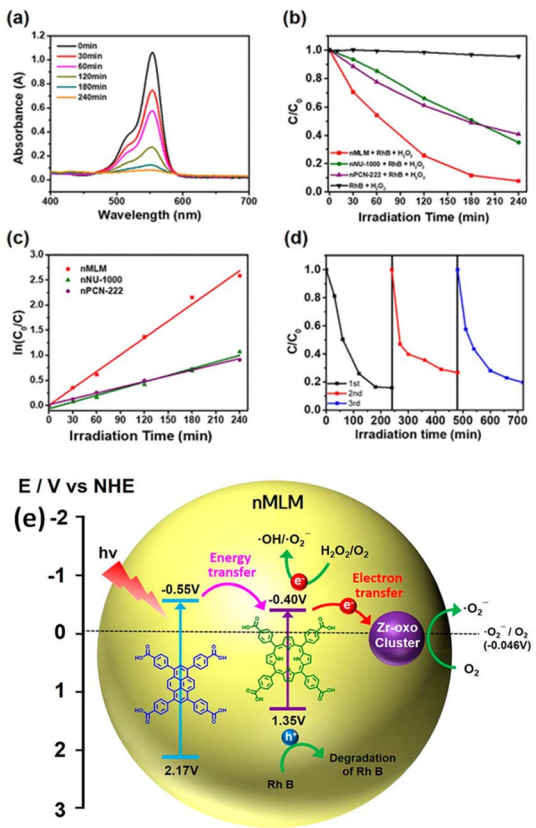

Fig. 7 (a) Absorption spectra of Rh B solution in the presence of H_2O_2 and nMLM; (b) visible-light photocatalytic degradation curve of Rh B over nMLM, nPCN-222, and nNU-1000; (c) kinetic study of the degradation process over nMLM, nPCN-222, and nNU-1000; (d) recycling test for nMLM; (e) proposed mechanism for rhodamine B (Rh B) degradation using nMLM.[157] This figure has been adapted from ref. 157 with permission from American Chemical Society, copyright 2020.

In addition, bimetallic MOFs have demonstrated a better understanding of selective dye removal through light irradiation. In this manner, a Fe–Co–BDC MOF was fabricated and employed to remove MB using peroxymonosulfate.[158] The MOF exhibited 100% dye degradation within 30 min, facilitated by peroxymonosulfate decomposition. Despite its relatively small surface area, this material displayed an effective dye degradation process due to several active sites of unsaturated Fe(II) and Co(II). There were also many reports of bimetallic MOF acting as a superior photocatalyst for degrading organic dyes.[159–161] In another study, a Cu(I)-based MOF was fabricated utilizing two triazole-based linkers with different molar ratios.[162] This unique MOF exhibited superior photocatalytic activity for the degradation of MB, Rh-B, MO, and sulfasalazine. The first MOF, CuMtz-1b, containing a significant amount of thiophene linker, displayed enhanced activity under the Xe lamp. In another report the self-assembly of 5-fluorine-3-(3,5-dicarboxylphenxoy) benzoic acid(H_3L) with cobalt(II) salts in absence as well as presence of a N-donor ancillary ligand 1,1′-(1,4-butanediyl) bis(imidazole)(bib) yields two new MOFs with formula $[Co_2(\text{-}\mu_3OH)(L)(H_2O)_3\ 2{\cdot}75H_2O]_n$ (1) and $[Co_2(\mu_3OH)(L)(bib)(H_2O)_2]_n$ (2).[163] The crystallographic study reveals that 1 exhibit only a 2D bilayer structure, while 2 displays an 8-connected node with a 3-periodic network. The photocatalytic activities of both MOFs have been tested for the degradation of MV, suggesting that 1 and 2 displayed efficient photocatalytic performances to degrade MV under UV irradiation. The mechanism has been proposed through band structure calculations. Another noteworthy MOF, JUC-138, fabricated by Zhao *et al.*, possesses anionic properties having pyrene organic linker and In(III) metal ion.[164] The experimental setup employed a mercury lamp UV light, and the degradation of Azur B was monitored for 1 h. Without JUC-138, only 30% degradation occurred, whereas, in the presence of JUC-138, the degradation reached 90%. Moreover, the catalyst demonstrated high stability and could be reused for multiple cycles. Another way one can enhance the photocatalytic performance of MOF is defective engineering. Inspired by this, researchers synthesized a series of defective MOFs, including ZnIr-MOF-d_x, by introducing Ir–BH_3 as a heteroatom linker into the parent MOF.[165] The role of defects in the photocatalytic degradation of Rh-B is truly astonishing. When exposed to light, ZnIr-MOF-$d_{0.3}$ achieved 100% photodegradation in 10 min. In contrast, the non-defective MOF exhibited only 34% degradation after 60 min. The enhanced photocatalytic activity of the MOF can be attributed to its mesoporous architecture and semiconductor behavior. Graphitic carbon nitride (g-C_3N_4) has been very popular due to its cost-effectiveness and high stability across different pH conditions, making it a promising material for better photocatalytic performance. However, its low surface area and quantum efficiency limit its effectiveness. In a study by Guo *et al.*, a composite of MIL-53(Al)/g-C_3N_4 was reported by mixing MIL-53(Al) with g-C_3N_4 under ambient conditions using the

sonication process.[166] The composite contained approximately 20% wt of g-C_3N_4 to achieve high photodegradation towards Rh-B. Inspired by these results, the fabrication of ZIF-8/g-C_3N_4 composite for the degradation of 10 ppm Rh-B under visible light has also been done. The ultrasonic method was employed to prevent the agglomeration of g-C_3N_4. The presence of ZIF-8 nanoparticles, which are chemically and thermally stable, grown on g-C_3N_4 significantly enhanced the photocatalytic performance. The composite indicates that the best results were observed when 3 wt% of ZIF-8 was employed. Increasing the weight of ZIF-8 beyond this point hindered the penetration of light onto the composite surface, thereby reducing the degradation efficiency.[167] Similarly, a composite based on g-C_3N_4, BiOCl/g-C_3N_4@UiO-66, demonstrated efficient degradation of Rh-B.[168] The synthetic procedure involves coating BiOCl/g-C_3N_4 on UiO-66, resulting in a composite that exhibited improved catalytic performance compared to g-C_3N_4 and the hybrid BiOCl/g-C_3N_4 alone. The high surface area of the composite is responsible for the reduced recombination rate of electron–hole pairs contributing to its efficiency reaching 99.9% in 1 h. Another approach is integrating MOF with graphene oxide (GO) through self-assembly. With its 2D architecture, and –OH and –COOH functional group is well-suited for better photocatalytic activity by accepting and transferring electrons. Chen *et al.*[169] employed this method to develop a Bi_2O_3/Cu-MOF/GO hybrid material for photocatalytic performance towards Rh-B in visible light. The synthetic process involves the dispersion of the appropriate amounts of Cu-MOF, GO, and Bi_2O_3 in DMF solvent. The composite exhibited enhanced stability due to the hydrogen bonds between the hydroxyl group of GO and the O atoms of Bi_2O_3 and Cu-MOF. The stability, coupled with the synergistic effects of different components, resulted in superior photocatalytic performance. The conductivity of GO, the adsorption properties of Cu-MOF, and the strong interaction of components contributed to enhanced photocatalytic performance. The Bi_2O_3 or binary Bi_2O_3/Cu-MOF hybrid material displayed inferior dye degradation, with only 90% degradation achieved in 2 h. Tang *et al.* fabricated a ZIF@rGO-based hydrogel for dye degradation. The process involved mixing an aqueous GO solution with ZIF-8 and heated for 1 h at 95 °C, followed by a freeze-drying process. The process enabled the distribution of Zn(II) ions in the active sites of graphene layers and the reduction of GO, facilitating self-assembly through π–π interactions.[170] Additionally, porphyrinic MOFs also governed much attention due to their superior photocatalytic activity. Chen *et al.* designed a MOF on the porphyrin ligand, with the chemical formula $[Me_2NH_2][Sr_2(TCPP)(OAc)(H_2O)]\cdot 2DMA$, where H_4TCPP represents tetrakis(4-carboxyphenyl)porphyrin, HOAc stands for acetic acid, and DMA represents *N*,*N*′-dimethylacetamide.[171] The designed MOF consists of two Sr^{2+} ions,

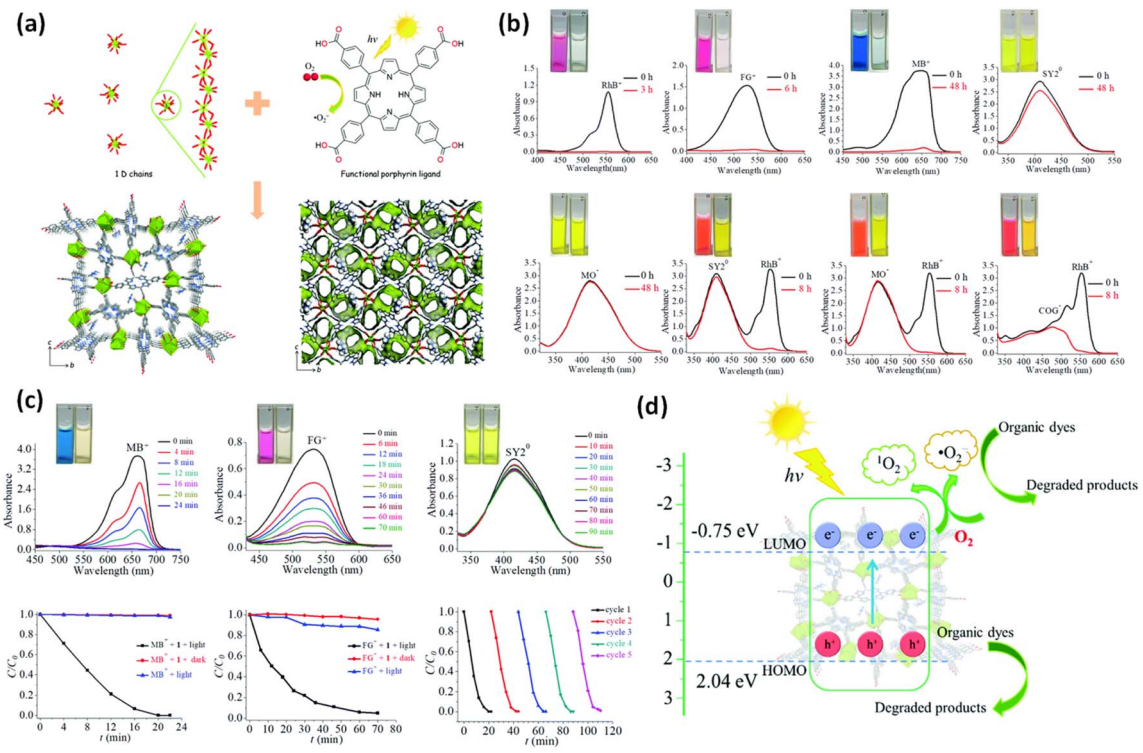

Fig. 8 (a) Infinite 1D chains, functional H_4TCPP ligand, 3D coordination framework, the 1D channels along the *a*-axis of **1**; (b) UV-vis absorption spectra for the adsorption experiments of organic dyes in acetonitrile solution, single component adsorption of RhB^+, FG^+, MB^+, SY2°, MO^- and two-component adsorption of RhB^+ and SY2°, RhB^+ and MO^-, RhB^+ and COG^-; (c) UV-vis absorption spectra of MB^+, FG^+, SY2° recorded at various times during the photocatalytic process, and the photocatalytic oxidation performance of **1** toward MB^+ and FG^+ and the reusability for photodegradation of MB^+; (d) the photocatalytic degradation reaction mechanism of organic dyes for **1**.[171] This figure has been adapted from ref. 171 with permission from Royal Society of Chemistry, copyright 2022.

each bound to two halves of $TCPP^{4-}$ ligands, water molecules, a counter cation $MeNH_2^+$, and guest molecules DMA. The coordination sphere of Sr_2 is occupied by eight O atoms from carboxylate, water, and $TCPP^{4-}$ ligands, forming a SrO_8 polyhedral SBU (Fig. 8a). To evaluate the solution state adsorption process, various organic dyes such as MB, crocein orange (COG), MO, the solvent yellow 2 (SY-2), basic orange 21 (BO-21), Rh-B, and FG were used. MOF 1 exhibited rapid adsorption of Rh-B, achieving almost 100% adsorption in just 3 h, whereas it took 6 h for FG (Fig. 8b). Furthermore, the MOF was also utilized for the photodegradation of anionic (MO), cationic (MB), and neutral (SY) dye. The MOF was immersed in different dye solutions, resulting in a quick color change for the MB solution, while the SY2 and MO solutions remained unchanged after 90 min of irradiation. UV-vis data revealed a decrease in the absorbance of MB, indicating efficient photocatalytic degradation with an efficiency of up to 99% within 22 min (Fig. 8c). To assess the recyclability of the MOF, a test was conducted for five consecutive cycles using MB. The plausible mechanism was also proposed which involves visible light absorption by the MOF, leading to the generation of h^+ and e^-. The LUMO of the MOF has a negative redox potential relative to $O_2/{}^{\bullet}O_2^-$, facilitating the reduction of O_2 into ${}^{\bullet}O_2^-$ and generating e^-. Consequently, the degradation of cationic dyes occurs through the involvement of ${}^{\bullet}O_2^-$, $^1O_2$, and h^+ (Fig. 8d). In another study, the author focused on 2-D MOFs based on porphyrin, which exhibited enhanced photocatalytic performance. These MOFs possessed a high surface area and porosity, contributing to their remarkable photocatalytic activity towards MO.[172] The UV-vis spectrophotometer was employed, suggesting the absorption peak of MO gradually decreased, achieving 46.2% efficiency within 60 min. The reaction followed first-order kinetics, with a reaction constant of 0.01 min^{-1}. Likewise, Hongwei Hou and colleagues synthesized six new isostructural MOFs that were named $\{[M_3(L)_2(4,4'\text{-bpy})_2(H_2O)_2]\cdot 14H_2O\}_n$. The author synthesized these MOFs with varying proportions of metal ions. The transition metals used in these MOFs are Co (1), $Co_{0.7}Ni_{0.3}$ (2), $Ni_{0.5}Co_{0.5}$ (3), $Co_{0.3}Ni_{0.7}$ (4), $Co_{0.1}Ni_{0.9}$ (5), and Ni(II) (6) and 1-aminobenzene-3,4,5-tricarboxylic acid as primary ligand. Under the Xe lamp, the catalytic activity of these MOFs, in the presence of H_2O_2, was evaluated for the degradation of four different dyes.

Among them, complex 1 exhibited the highest photocatalytic activity, suggesting introducing Ni(II) ions into the MOFs decreased its photocatalytic performance significantly. This observation highlights the controllable regulation of photocatalytic activity by replacing the metal ion, while 1 displayed superior photocatalytic activity for degrading MO, MB, Rh-B, and gentian violet (GV).[173] Some toxic metal-based MOFs have also been explored in the photocatalytic degradation of organic dyes. Subsequently, a report by Kumar *et al.* focuses on designing Pb(II)-based 2-D bilayer MOF, which exhibited seamless photocatalytic activity towards MO. The theoretical study was conducted by the density of states (DOS) and partial density of states (p-DOS).[174] The DOS and p-DOS revealed a significant contribution from the VB located at the Fermi level, primarily from carboxylate O and other ligands. The CB was positioned just above the Fermi level, ranging from −1.4 to −0.6 eV, due to the presence of N in the tetrazole moiety.

Also, electronic transitions occurred from the carboxylate group with aromatic centers to the tetrazole moiety, facilitating the ligand-to-ligand charge transfer. The band structure calculations indicated that the material could be excited to generate e^-–h^+ under visible light. The h^+ would then migrate towards the carboxylate group with aromatic centers, while the electron would migrate to the tetrazole moiety.[174] Another approach is employing core–shell MOFs, combining two different MOF structures to tackle significant challenges.[39] Zhou *et al.* derived a core–shell structure based on ZnO nanomaterial and ZIF-8. The carbonization of the material follows the initial synthesis of ZnO-ZIF-8 to obtain a carbon material. The sacrificial ZnO nanorods provided a template for achieving a tightly bound ZIF-8 structure, and the thickness of the carbon layer was controlled by manipulating the ligand. This converts the ligand into nano-sized ZnO particles encapsulated in the porous carbon matrix. The pyrolysis process increased its surface area and facilitated the transport of charged species.[39] The ZnO-nZnO@PC composite was then employed as a photocatalyst for the degradation of the MB under UV-visible light. The catalytic activity of the composite varied with different thicknesses of the carbon layer coated with ZnO. The Zn-nZnO@PC composite with a ZnO-to-ligand ratio of 1 : 0.5 (denoted as $ZZPC_{0.5}$) exhibited high degradation efficiency in MB. However, as the thickness of the carbon layer increased, the catalytic activity decreased due to the shielding effect and unnecessary recombination caused by an excessive carbon layer (Fig. 9).

In a study, two MOFs were designed and extensively characterized with some spectral techniques. The one material is basically a 2D MOF and the other one is basically 1 3D MOF incorporating two linkers. When the photocatalytic activities of these MOFs were evaluated, they demonstrated enhanced photodegradation towards MV dye. Upon comparing the photocatalytic performances, the 2-D MOF exhibited superior activity. Again the mechanism was investigated through DOS and p-DOS calculations.[175] The VB exhibited significant contributions from aromatic carbons and carboxylated O in both MOFs. The 3D MOF showed contributions from the N centers of the bpy ligand, but no contribution occurred by Zn(II) ion. The aromatic C and N atoms in both MOFs mainly provided the CB. The p-DOS determined the electronic transitions within the MOFs followed by ligand-to-ligand transfer. The disparity in photocatalytic performance could be attributed to their different bandgap energies. Additionally, the presence of bpy in 3D MOF likely contributed to its higher photocatalytic efficiency which also suggest by some recent literature.[159,176,177] A compilation of recent reports on the degradation of organic pollutants employing MOF can be found in Table 3.

3.3 Polyoxometalate (POM) based MOFs for degradation of organic pollutants

Polyoxometalates (POMs), a subclass of polyoxoanions, primarily consist of very early transition metal ions, namely Mo and W. They were initially discovered in the late 19th century,

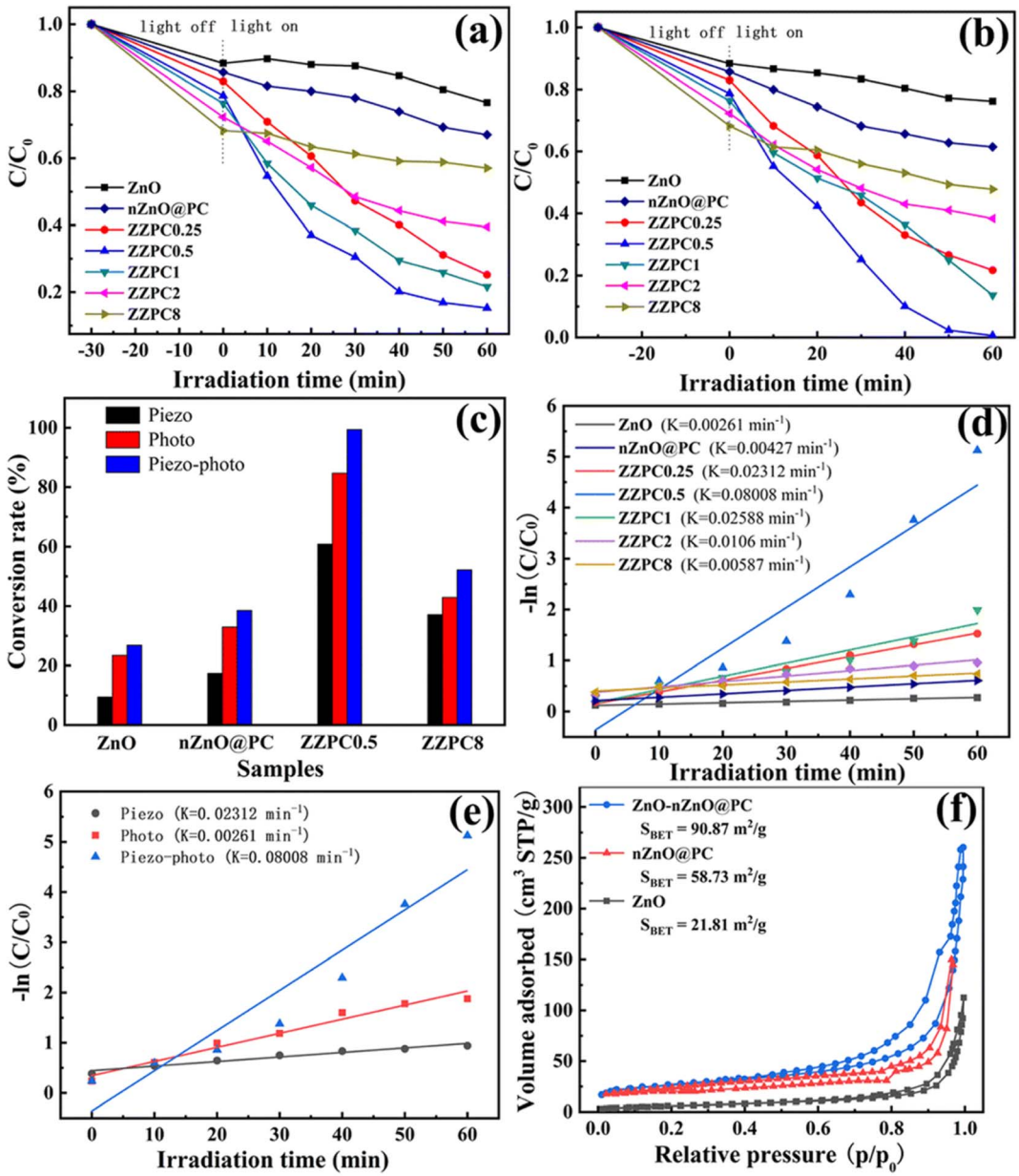

Fig. 9 The (a) photocatalytic and (b) piezo-photocatalytic degradation of MB by ZnO, nZnO@PC, and the ZnO-based core–shell structure; the (c) comparison result of piezo-, photo-, and piezophoto-catalytic of ZnO, nZnO@PC, and ZnO-nZnO@PC; the kinetic fits correspond to the (d) piezo-photocatalytic degradation performance and (e) performance under different stimulations of ZnO, nZnO@PC, and ZnO-nZnO-PC core–shell structures; the (f) N2 adsorption–desorption isotherms of ZnO, nZnO@PC, and the optimal ZnO-nZnO-PC.[39] This figure has been adapted from ref. 39 with permission from Royal Society of Chemistry, copyright 2023.

but it is in recent decades that their prominence has grown due to the utilization of modern experimental techniques to investigate their exact structure.[197,198] POMs are widely accepted for their versatile applications as metal oxide or clusters.[199] Apart from having various structural features, the POMs possess brilliant physiochemical properties that make them ideal candidates for various applications, including magnetism, energy storage, photo, and electrocatalysis. The recent literature suggests that POMs are highly promising candidates for the photocatalytic degradation of organic pollutants, thanks to properties resembling those of semiconductor materials, which have been extensively utilized in photocatalysis. These materials offer several advantages in the photocatalysis process. Firstly, POM-based materials are rich in early transition metal ions, providing a wide range of potential active sites. Secondly, POMs can be easily functionalized with other conductive materials, enabling synergistic interactions. Given the inherent photo redox behavior typically observed in POM-based MOFs, numerous instances of redox-active MOFs designed for the adsorption of organic pollutants have been documented in scientific literature.[200–203]

Table 3 Overview of the key information of MOFs and MOF composites found in literature related to the catalytic degradation of organic dyes

Dye	MOF materials	Catalytic efficiency (%)	Reaction conditions	Ref
AB	JUC-138	(90)	4 h, 400 W Hg	164
B41	MIL-100(Fe)	(99–98)	180 min, 15 ppm, pH = 5	178
B41	MOF-199	(~100%)	180 min, pH = 2–10	179
BG	MIL-101(Cr)@rGO-Pd	(100)	15 min	180
MB	Cd-TCAA	(81)	171 min, 500 W Xe	181
MB	CuTz-1	(100)	8 min, RT, + H_2O_2, 300 W Xe	182
MB	HPU-3	(97.2)	60 min, + H_2O_2	183
MB	HPU-4@AgBr	(95)	60 min, 12.75 ppm, 300 W Xe	184
MB	MIL-53	(11)	40 min, UV	185
MB	MIL-88B(Fe)-NH_2@TiO_2 (SU-3)	(100)	2.5 h, 50–150 ppm, pH = 2–8, + H_2O_2, 5 W LED	186
MB	MIL-88B(Fe)@BiOI	(80)	80 min, 300 W Xe	187
MB	MIL-88B@BiOI/$ZnFe_2O$	(73.8)	120 min, 10 ppm, 25 °C, LED	188
MB	MIL-88B(Fe)-NH_2@g-C_3N_4	(100)	120 min, 30 ppm + H_2O_2, 500 W Xe	189
MB	MIL-100(Fe)33%@TiO_2	(~100)	60 min, 50 ppm, + H_2O_2	190
MB	MIL-100(Fe) and Fe-BTC	(100)	60 min, 30–70 °C pH = 3–7, + H_2O_2	191
MB	MIL-100(Fe)@FeII	(91)	25 h, + H_2O_2	192
MB	MIL-101(Fe)@Ag/AgCl/	(99.75)	10 ppm, pH = 7, + H_2O_2, 500 Xe	193
MB	UiO-66-NH_2@ZnTCPc	(68)	120 min, 500 W Xe	194
MB	UiO-66@α-Fe_2O_3	(100)	55 min, 0.04 mM, 300 W	195
MB	ZIF-8	(83.2)	120 min, 10 ppm, pH = 4–12, 500 W Hg	196

Furthermore, the band gap energy between these materials can be readily tuned by altering the heteroatoms.[204–206] However, there are two main drawbacks associated with POM-based photocatalysts. Their high solubility in aqueous mediums and limited activity under low visible light irradiation.[207] It has been reported that only 5% of sunlight can be effectively utilized by POMs, which hampers their claims of high photocatalytic efficiency. Recent research has focused on modifying POMs into hybrid materials for better photocatalysis.[204] One approach involves fabricating novel materials by incorporating POMs with metal oxides and carbides, resulting in a uniform structure.[208] Other methods involve POMs with other porous

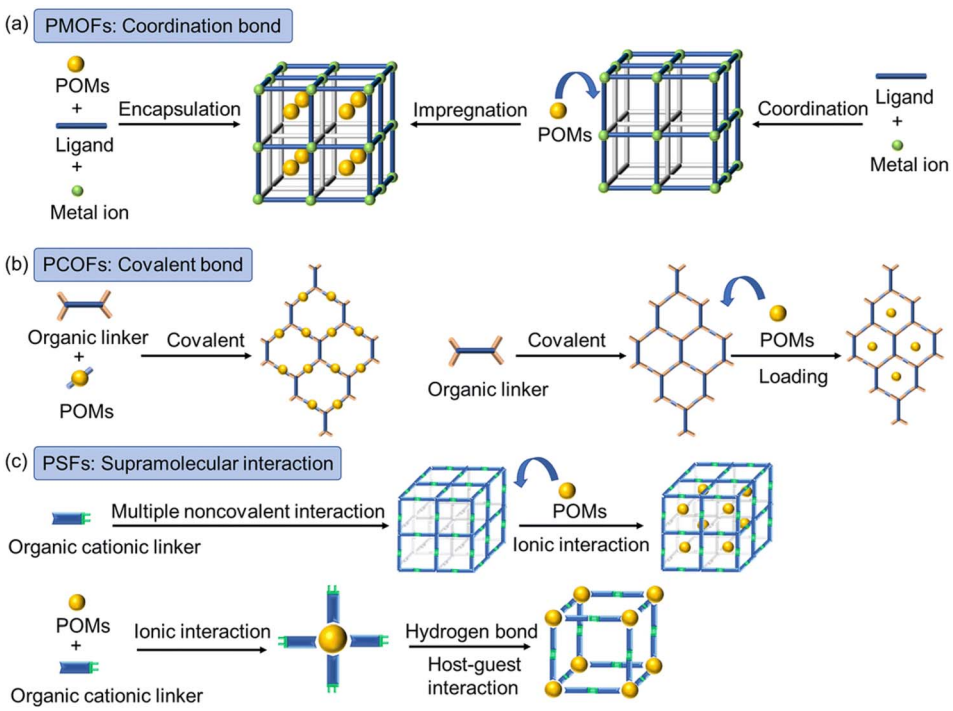

Fig. 10 Synthesis strategies and interactions for constructing (a) POM-based metal–organic frameworks (PMOFs); (b) POM-based covalent–organic frameworks (PCOFs); and (c) POM-based supramolecular frameworks (PSFs). Frames of MOFs: black and grey sticks; COFs: blue and orange sticks; organic linkers in SFs: green-blue bicolored sticks; metal ions: green spheres; POMs: dark yellow spheres.[216] This figure has been adapted from ref. 216 with permission from Royal Society of Chemistry, copyright 2023.

materials, such as MOFs or COFs, which enhances catalysis and product selectivity.[209] Specifically, POM-based MOFs are primarily synthesized through coordination bonds between N and O-donor organic linkers connected with POMs.[210] For instance, Liu *et al.* utilized Keggin POMs to facilitate the construction of Ni^{2+} with bpy, establishing an open POM-based MOF.[211] Lan *et al.* demonstrated the design of a stable framework by linking Zn-terminated ε-Keggin POMs with organic linkers.[212] In some cases, POMs are incorporated as guest molecules within MOF cavities (Fig. 10a). In this scenario; POMs are not considered as part of the frameworks but rather embedded within the pore of MOFs, with MOFs acting as the host and POMs as the guest molecule.[213] In addition, there are reported cases of POM-based COF materials where a coordination architecture is formed between POM and the organic building block through covalent linkages (Fig. 10b).[214] Additionally, there have been instances of supramolecular frameworks (SFs) that exhibit strong noncovalent interactions with POMs.[215] There were several noncovalent interactions driven by PMOFs, PSFs, and PCOFs are observed (Fig. 10c). While these PSFs and PCOFs exhibit diverse structural features for functional applications, their application in photocatalytic activity is still in its nascent stage. Consequently, PMOFs have gained popularity so we will focus solely on them in this discussion.

We have harnessed the potential of POMs as an encapsulation strategy within MOFs, a promising avenue for enhancing the functionality of these materials. This encapsulation approach holds substantial promise for a variety of applications, particularly in the realm of adsorption and photocatalytic degradation of organic pollutants. However, to fully comprehend the transformative impact of this strategy, it is essential to delve deeper into the host–guest interaction dynamics that underlie it.[217] Host–guest interactions represent a critical facet of POM-based MOF composites and are undeniably instrumental in elucidating the mechanisms responsible for their enhanced performance. These interactions intricately govern the adsorption capacity and photocatalytic efficiency of these hybrid materials, and thus, warrant comprehensive examination.[218] These interactions manifest when the MOF, acting as the host framework, accommodates POM molecules as guest species within its porous structure. The synergy between the host MOF and guest POM is underpinned by various molecular forces, including electrostatic interactions, hydrogen bonding, and van der Waals forces. Enhanced adsorption capacities result from the cooperative action of these forces, enabling the MOF–POM composite to capture and retain organic pollutants effectively.[219] Moreover, host–guest interactions influence the composite's photocatalytic activity by influencing charge transfer processes and the lifetime of photogenerated species. Therefore, a comprehensive understanding of these intricate interactions is paramount for harnessing the full potential of POM-based MOF hybrid materials in photocatalytic degradation and adsorption of organic pollutants.[220]

Inspired by these concept several POM-based MOFs to exhibit high photocatalytic activity.[209] Maggard *et al.*, has designed three silver-vanadate-based materials: $Ag_4(pzc)_2V_2O_6$, $[Ag(4,4'\text{-bpy})]4V_4O_{12}\cdot 2H_2O$, and $[Ag(dpa)]_4V_4O_{12}\cdot 4H_2O$. These materials exhibit enhanced photodegradation performance towards MB in UV-visible light.[221] The synthetic process involved neutral $[Ag_4V_4O_{12}]_n$ layered pillars bonded to 4,4′-bpy ligands at each Ag site (Fig. 11a and b). The presence of heterometallic oxide with d^0 and d^{10} configurations typically results

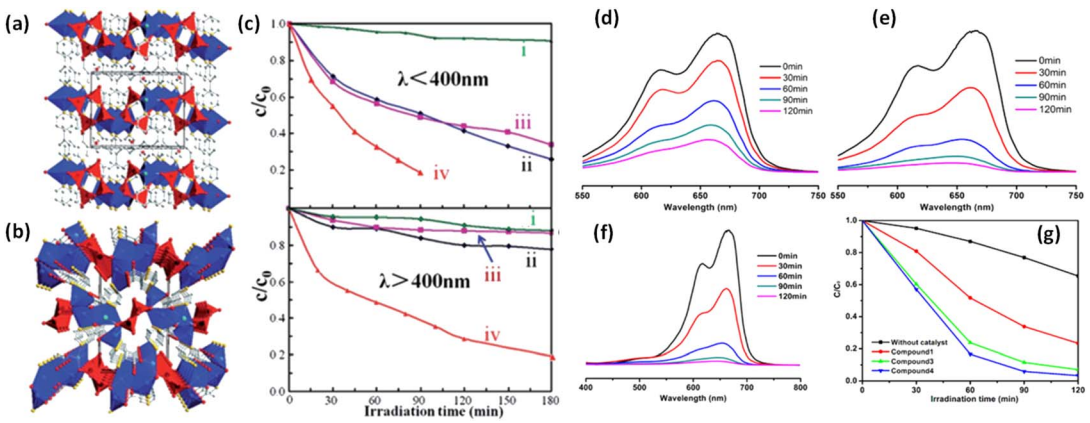

Fig. 11 (a) Structures of $[Ag(4,40\text{-bpy})]_4V_4O_{12}\cdot 2H_2O$ viewed down the [001] direction of the unit cells (outlined). Blue polyhedra = Ag centered coordination environments, red polyhedra = VO_4, red spheres = O, yellow spheres = N, white spheres = C, and light-blue spheres = Ag; (b) polyhedral structural view of $Ag_4(pzc)_2V_2O_6$ down the [100] direction of the unit cell (outlined). Blue polyhedra = Ag centered coordination environments, red polyhedra = VO_5, red spheres = O, yellow spheres = N, white spheres = C, and light-blue spheres = Ag. All H atoms are omitted for clarity; (c) photocatalytic decomposition of MB solutions (6.0 mg L^{-1}, 50 mL) using 150 mg of the three silver vanadates, either under UV (upper) or under visible-light (lower) irradiation for $[Ag(4,40\text{-bpy})]_4V_4O_{12}\cdot 2H_2O$(II), $[Ag(dpa)]_4V_4O_{12}\cdot 4H_2O$(III), $Ag_4(pzc)_2V_2O_6$, (iv) photolysis of MB without the use of the photocatalysts.[221] This figure has been adapted from ref. 221 with permission from American Chemical Society, copyright 2008; (d–f) UV-vis absorption spectra of the MB solution during the decomposition reaction under UV light irradiation in the presence of **1**, **3**, and **4**. (g) Plot of irradiation time *versus* concentration for MB under UV light in the presence of the compound **1**, **3**, and **4**, and the black curve is the control experiment without any catalyst.[223]. This figure has been adapted from ref. 223 with permission from American Chemical Society, copyright 2013.

in a smaller bandgap energy, enabling efficient utilization of visible light for initiating the photocatalytic activity.[222] The optical band gap energies of the three MOFs mentioned above were determined using the DRS method. The $[Ag(4,4\text{-bpy})]_4V_4O_{12}\cdot 2H_2O$ exhibited a band gap energy of 2.77 eV, while $[Ag(dpa)]_4V_4O_{12}\cdot 4H_2O$ had 2.95 eV. On the other hand, the $Ag_4(pzc)_2V_2O_6$ displayed a lower band gap energy of 2.45 eV. These band gap energies indicate the photocatalytic activity of these MOFs is primarily confined to the UV region. Among the MOFs, $Ag_4(pzc)_2V_2O_6$ demonstrates effectiveness in the UV-visible range, owing to its lower band gap energy. This unique characteristic enables $Ag_4(pzc)_2V_2O_6$ to efficiently degrade the MB, with an impressive 80% reduction achieved within 180 min (Fig. 11c). This suggests the combined effect between Ag-oxide/organic chains and the vanadate facilitates the transportation of h^+ and e^- to the surface for enhanced photocatalytic performance. Overall, the results highlight the practicality of the combined effect in $Ag_4(pzc)_2V_2O_6$, contributing to its superior photocatalytic performance compared to the other MOFs. Subsequently, Ma *et al.* conducted a study where they synthesized four MOFs: $[CuI_2(1,3\text{-btp})_2][CuI_2(trans\text{-}1,3\text{-btp})_2Mo_6O_{18}(O_3AsPh)_2]$ (1), $[CuI_4(1,4\text{-btp})_4Mo_6O_{18}(O_3AsPh)_2]$ (2), $[CuI_4(1,5\text{-btp})_4Mo_6O_{18}(O_3AsPh)_2]$ (3), and $[CuI_4(1,6\text{-bth})_2Mo_6O_{18}(O_3AsPh)_2]$ (4) for better photocatalytic performance. These MOFs comprised of $[Mo_6O_{18}(O_3AsPh)_2]_4$ units combined with copper and organic ligands.[223] The bandgap energies of these MOFs were determined using DRS and found to be 2.6 eV, 2.7 eV, 2.1 eV, and 1.9 eV, respectively. The photocatalytic performance of these MOFs was then evaluated for the degradation of the MB. MOFs 1, 3, and 4 dispense efficiencies of 76%, 93%, and 97%, respectively, while MOF 2 did not demonstrate any appreciable change in the dye solution. It is worth noting that MOFs 1, 2, and 3 have a 3-D structure, but the prolonged As_2Mo_6-containing units in MOF 1 differ from those in MOF 2 and 3. On the other hand, MOFs 3 and 4 possess a 3-D structure with a polycatenated framework known as a 3D tetranodal

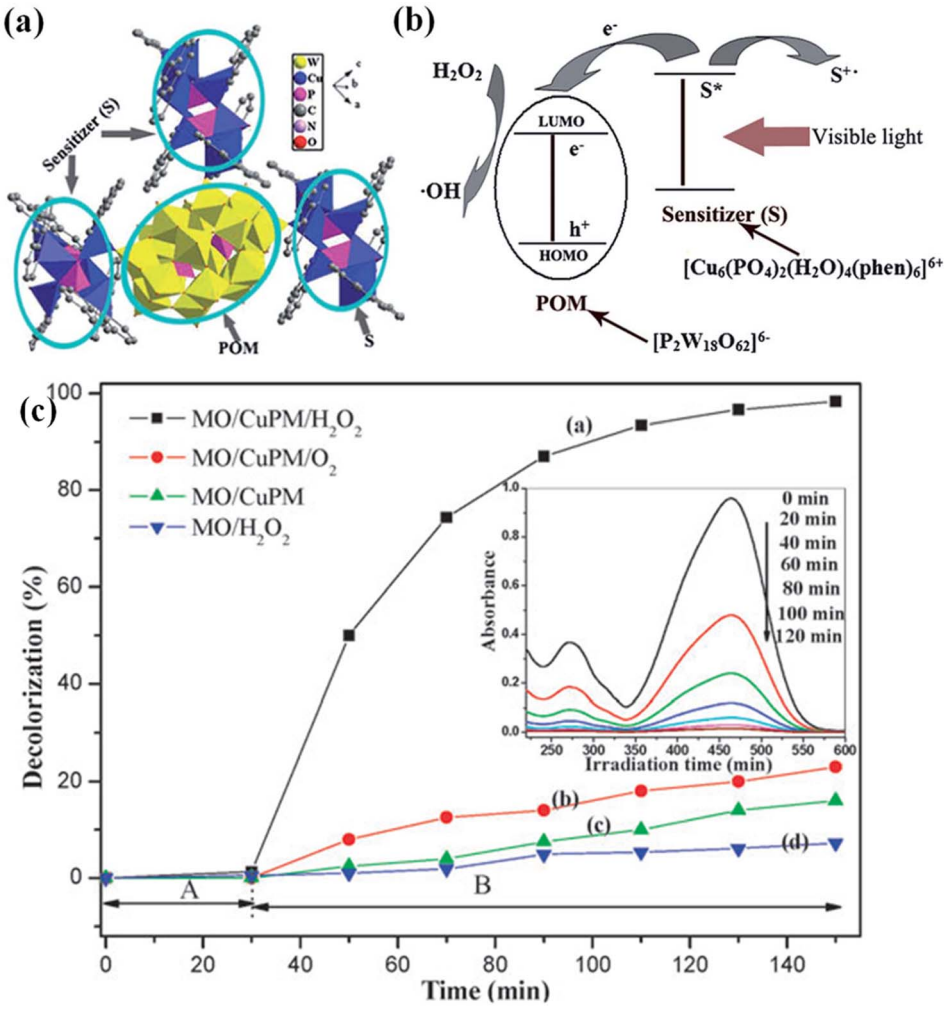

Fig. 12 (a) Relationships between the hexacopper phosphate cluster as the sensitizer and the Wells–Dawson polyoxoanions as the POM unit in CuPW; (b) proposed photodegradation mechanism on CuPM; (c) decolorization rates of MO in different reaction systems. Initial concentrations: MO (15 mg L^{-1}, pH = 2.5), CuPM (0.5 g L^{-1}), H_2O_2 (1.5 mmol L^{-1}), MO/CuPM/H_2O_2, MO/CuPM/O_2, MO/CuPM, MO/H_2O_2. Inset shows UV/vis spectral changes of MO solution under visible light irradiation corresponding to curve a.[224] This figure has been adapted from ref. 224 with permission from Royal Society of Chemistry, copyright 2010.

(3,4,6)-connected architecture. The photocatalytic performance of MOF 3 and 4 is effective due to the distribution of As_2Mo_6 polyoxoanions throughout. As a result, MOFs 1, 3, and 4, which feature more comprehensive 3-D As_2Mo_6 frameworks, exhibit superior photocatalytic activity (Fig. 11d–f). This comprehensive As_2Mo_6 framework facilitates the transportation of holes and electrons on the surface, initiating the photodegradation of MB (Fig. 11g).

A study by Cao *et al.* involves the synthesis of a new POM-based MOF with the chemical formula $[Cu_6(PO_4)_2(H_2O)_4(phen)_6(CuPW)]$ by combining hexacopper phosphates and Wells–Dawson POMs, exhibited remarkable catalytic degradation of MO.[224] Analysis of the electronic spectra revealed a broad absorption band at 690 nm in the POM-based MOF, resulting from charge transfer between $(P_2W_{18}O_{62})_6$ and $[Cu_6(PO_4)_2(H_2O)_4(phen)_6]^{6+}$. Additionally, $[Cu_6(PO_4)_2(H_2O)_4(phen)_6]^{6+}$ acted as a sensitizer under visible light irradiation (Fig. 12a and b). The electron transfer occurred from the sensitizer to the LUMO energy level $(P_2W_{18}O_{62})_6$. The POM core was an electron reservoir, allowing electron reduction without hampering it. In this context, the adsorbed H_2O_2 readily trapped electrons in the LUMO of the anionic POM, generating $^{\bullet}OH$ that effectively cleaved the dye (Fig. 12c). It is worth mentioning that coordinating POMs with lanthanide metals is another concept making a lot of recognition.[225] The diverse coordination capabilities and unique optical properties of lanthanides make these materials promising for the photodegradation of organic dyes.[226] In this regard, the research group of Chen published their findings on Keggin heteropolymolybdate-based MOFs, including $[2,6\text{-pdc}]_3(PMo_{12}O_{40})$, $[Sm(H_2O)_4(2,6\text{-pdc})]_3Sm(H_2O)_3(2,6\text{-pdc})\cdot 3H_2O$ and $[La(H_2O)_4(2,6\text{-pdc})]_4(PMo_{12}O_{40})F$, which exhibited enhanced degradation of Rh-B.[227] The latter two MOFs demonstrated higher degradation efficacy than the first, suggesting that adding Ln(III) ions in POM-based MOFs enhances their photocatalytic activity, comparable to TiO_2-based materials. Moreover, it was observed that Ln(III) ions acted as electron trappers in the UV region within the latter two MOFs, reducing the recombination rate of photogenerated electron–hole pairs and increasing the quantum yield.[228] Additionally, Wang *et al.*, explained the addition of lanthanide ions which could inhibit the photodegradation of Rh-B in a series of MOFs, namely $[Ce(2,5\text{-Hpdc})(2,5\text{-pdc})(H_2O)_6\{Ce(2,5\text{-}H_2pdc)_{0.5}(\alpha\text{-}PW_{11}O_{39}H)Ce(H_2O)_4\}]_2\cdot 12H_2O$, $[La(2,5\text{-Hpdc})(2,5\text{-pdc})(H_2O)_6La(2,5\text{-}H_2pdc)_{0.5}(\alpha\text{-}PW_{11}O_{39}H)La(H_2O)_4]_2\cdot 8H_2O$, and $[Pr(2,5\text{-Hpdc})(2,5\text{-pdc})(H_2O)_6Pr(2,5\text{-}H_2pdc)_{0.5}(\alpha\text{-}PW_{11}O_{39}H)Pr(H_2O)_4]_2\cdot 8H_2O$.[229] The proposed mechanism suggests that when UV light is absorbed by MOF, the H-bonding and weak π–π interactions between the MOF and Rh-B increase the chemical stability, prohibiting its high photocatalytic performance.

In another publication, Zhu *et al.* presented the design of a porous molybdophosphate-based $Fe^{II,III}$-MOF, through a hydrothermal process.[230] The material underwent thorough characterization, including single-crystal X-ray analysis. The porous nature of the POM contributed to the selective degradation of Rh-B. The POM demonstrated recyclability up to 4 times and achieved effective degradation of Rh-B within 3 h due to its high-water stability. Additionally, incorporating a POM into the cavities of a Zr(IV)-MOF enhances photocatalytic performance.[231] The research group led by Mia Du reported the PSM of MOF with a POM, which enhanced the water stability of the parent material. The hybrid material demonstrated excellent photocatalytic activity for Rh-B with 99% efficiency in the presence of H_2O_2 and stability up to three cycles.[232] Similarly, Chen *et al.* also constructed a POM-based MOF and evaluated its photocatalytic performance. The hybrid material exhibited superior photocatalytic degradation of MB and Rh-B under visible light.[233] Furthermore, many reports in the existing literature offer valuable insights into the strategic design of POM-based MOF materials aimed at enhancing photocatalytic performances.[234–236]

3.4 Theoretical aspect of MOF-based photocatalytic materials

Computational studies based on quantum mechanics are essential to gain insights into the photocatalytic mechanisms of MOFs and their composites. One of the most widely used computational methods is the Kohn–Sham density functional theory (KS-DFT), which offers high accuracy and computational efficiency.[237] KS-DFT approximates the exchange–correlation function, which determines the electronic exchange–correlation energy density at different points based on features such as electronic kinetic energy densities, electronic spin densities, and gradients. Hybrid functionals can incorporate the Hartree–Fock exchange, making the exchange and correlation energy nonlocal by considering the integral space.[238] Quantum mechanical (QM) calculations, including KS-DFT, have been employed to study photocatalytic electronic properties of MOFs and reaction mechanisms due to their complex chemical structures. These calculations can elucidate the excited state of the material's behavior and reaction mechanisms. The KS-DFT also provides information about the bandgap energy by calculating the difference in orbital energies in the ground states, specifically the difference between the lowest unoccupied crystal orbitals (LUCO) and the highest occupied crystal orbitals (HOCO).[239] On the other hand, time-dependent density functional theory (TD-DFT) can be employed for the linkers present in MOFs with the aid of the linear response approximation. TD-DFT also allows calculations of excited states and electronic transitions, providing valuable information about the optical properties and absorption spectra of MOFs.[239] Indeed, cluster-based MOFs can also be investigated using a DFT. The widely explored Perdew–Burke–Ernzerhof (PBE) functionals can be used to study the electronic properties and mechanisms associated with the photocatalytic behavior of MOFs. However, it is important to note that the PBE functionals may not accurately predict the band gap or the optical properties of MOF, but the hybrid functions are more suitable for such predictions.[240] Although more precision is needed in predicting the optical properties and bandgap energies, hybrid functional models can be computationally expensive when applied to complex structures, which hinders their widespread use. For example, the bandgap energy of UiO-66(Zr) was estimated using both PBE

and HSE06 functionals, and it was found that the empirically calculated bandgap energy differed from that predicted value by PBE functionals. Hybrid functionals such as HSE03 and HSE06 have been applied to estimate bandgap energies of photoactive MOFs like MOF-5, UiO-66(Zr), HKUST-1, UiO-67(Zr), and ZIF-8. Local functionals like HLE17 have shown higher accuracy compared to older functionals.[241] On the other hand, machine learning (ML) has also gained significant attention for predicting the properties of various energy materials.[242–244] The combination of ML with DFT has been pathbreaking in predicting metallic properties and demonstrates brilliant application in materials science. At the same time, ML has not been extensively explored for predicting the photocatalytic mechanisms but holds promise as a tool for designing efficient photocatalytic MOFs.[245] It is worth noting that while PBE functionals have been widely used for predicting bandgap energies of MOFs, they can sometimes underestimate the bandgap energy of semiconductors, leading to inaccurate predictions related to electrical conductivity.[246] In heterogeneous photocatalysis, two fundamental limits are interconnected: the production of charge carriers through light irradiation and the underlying mechanism of light absorption. Secondly, the movement of electrons and holes on the surface often conflicts with recombination in the bulk surface. Additionally, the reaction is initiated by the interaction of electrons and holes, as illustrated in Fig. 13a.[247] The well-defined architectures of MOF offer a significant advantage in the computational design of novel MOF-based photocatalysts.[248] One prominent example is the isoreticular IRMOF-1 (MOF-5), with the chemical formula $Zn_4O(BDC)_3$, where BDC^{2-} represents 1,4-benzene dicarboxylate. This MOF was among the first to undergo such processes.[249] Fuentes-Cabrera and colleagues researched the electronic structure of these MOF structures using LSDA functionals.[250] Their study revealed that the p states of C and O dominate the LUCO in the ligand, while the p states of the Zn_4 cluster and the C and O in the ligand influence the highest HOCO. The calculated band gap energy was approximately 3.5 eV, near the experimental values of 3.4–3.5 eV.[143,144]

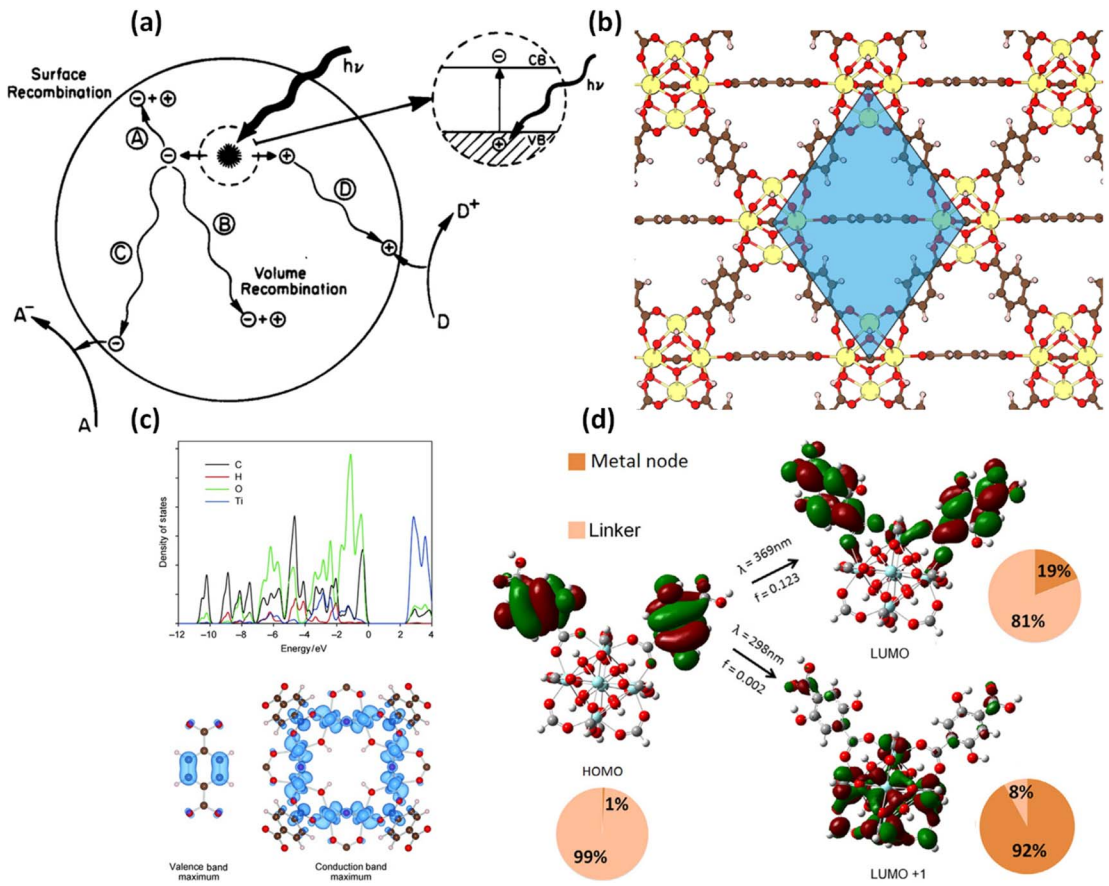

Fig. 13 (a) The basic processes in a heterogeneous photocatalysis system.[247] This figure has been adapted from ref. 247 with permission from American Chemical Society, copyright 1995; (b) framework structure of UiO-66(Zr) with the primitive cell indicated in blue (Zr, yellow; O, red; C, brown; H, light pink).[263] This figure has been adapted from ref. 263 with permission from American Chemical Society, copyright 2018; (c) PBE-calculated projected density of states for MIL-125(Ti) (upper panel) and density isosurfaces (in blue) for valence band maximum (HOCO) and conduction band minimum (LUCO) of MIL-125(Ti) (Ti, blue; O, red; C, brown; H, light pink).[257] This figure has been adapted from ref. 257 with permission from Willey, copyright 2010; (d) schematic view of the first and second excitations of the cluster model $[Zr_6O_4(OH)_4(HCOO)_{10}$(HBDC-2,5$(OH)_2)]$ of doubly functionalized UiO-66(Zr) with OH (Zr, cyan; O, red; C, gray; H, white).[261] This figure has been adapted from ref. 261 with permission from American Chemical Society, copyright 2015.

When a different computational program, such as PBE or PBE_{sol}, was applied to IRMOF-1, the author obtained comparable HOCO, LUCO, and band gap values.[251] It was suggested that substituting the metal ion is another promising strategy for manipulating the electronic properties of MOFs. However, in the case of IRMOF-1, the band gap energy remains relatively constant at around 3.5 eV, regardless of the substitution with various metal ions.[250,252] However, when the central O in the IRMOF-1 cluster is replaced with S, Se, or Te, the band gap can be readily tuned in the sequence O → S → Se → Te, resulting in a sequential decrease to approximately 2.5 eV. The influence of metal substitution such as Zn by Cd, Be, Mg, Ca, Sr, or Ba also enhances this effect.[253] Additionally, substituting the linker with halogen atoms reduces the band gap energy by 0.2 to 0.8 eV.[135] Kuc and colleagues studied the electronic properties of IRMOFs, which share the same Zn_4O node but have different organic ligands.[254] The author discovered that more extended ligands and those with greater conjugation exhibit larger band gap energies. Similar findings were summarized by Valenzano *et al.*, who investigated $(Zr_6O_4(OH)_4(BDC)_6$ (UiO-66(Zr)), a photocatalytic MOF known for its extra stability (Fig. 13b) and an experimentally measured band gap in the range of 3.76–4.07 eV.[255] Doping of metals and functionalization of ligands with various functional groups (such as NH_2, NO_2, and I) are two different approaches for tuning the electronic structure of UiO-66 materials, enabling targeted reactions, and achieving visible-light absorption and efficient charge separation.[174] Furthermore, there is a notable trend in the band gap energy decrease from UiO-66(Zr) to UiO-67(Zr) to UiO-68(Zr),[256] which is also observed in IRMOFs.[254] Subsequently, Walsh *et al.* investigated the electronic properties of MIL-125(Ti) with the chemical formula $Ti_8O_8(OH)_4(BDC)_6$. Their study indicates the HOCO is predominantly governed by the 2p states of C and O, while the LUCO is dominated by the Ti 3d-O 2p-hybridized states of TiO_2 units, as shown in Fig. 13c.[257] As previously reported for UiO-66(Ce), achieving spatial charge separation with electron localization on the metal ion and linker hole localization is attainable in MOFs. In another study, Nasalevich and colleagues conducted electron paramagnetic resonance (EPR) and transient absorption spectroscopy on MIL-125(Ti) and UiO-66(Zr), suggesting that MIL-125(Ti) exhibits a slightly longer excited state. Metal doping and ligand functionalization have shown promise in tuning the electronic properties of MIL-125(Ti).[139,258,259] Addition to that, Wang *et al.* synthesized a new MOF called Ti-MOF (MIL-177), which surpasses MIL-125(Ti) in various aspects. Jiao *et al.* reported numerous MOF-based composites involving Fe/W co-doped $BiVO_4$ photoanodes and MIL-100(Fe) acting as cocatalysts. *In silico* studies of these MOFs exposed the presence of minor impurities that enhance light absorption and ultimately promote efficient photocatalytic activity.[260] Photoexcitation is a crucial process in photocatalysis, and it can occur through four main mechanisms: (i) ligand-localized excitation, (ii) localized excitation of nodes, (iii) ligand-to-metal charge transfer (LMCT) excitation, and (iv) metal-to-ligand charge transfer (MLCT) excitation. Hendrickx and colleagues conducted a TD-DFT study on UiO-66(Zr) with a ligand arrangement including OH, utilizing a cluster model $[Zr_6O_4(OH)_4(HCOO)_{10}(HBDC^{-2},5(OH)_2)]$.[261] Their study revealed that the ligand undergoes localized excitation through a π–π* transition when excited at 369 nm, while the LMCT excitation occurs at 298 nm, albeit with low oscillating strength (Fig. 13d). The TD-DFT results demonstrate that functionalizing UiO-66(Ce) shows stronger ligand-localized excitation than LMCT and node-localized excitations.[262] Therefore, the photoexcitation behavior of UiO-66 with Zr and Ce versions exhibits similar characteristics. A recent study by Hendrickx and colleagues investigated the photoexcitation of UiO-66(Zr) with Ti-doping suggests they identified a peak contribution from the localization of exciting nodes in the excitation spectrum after incorporating Ti-doped material. Furthermore, when amino-functionalization is applied to UiO-66(Zr/Ti), even LMCT excitation can play a non-negligible role in the excitation spectrum.

4. Concluding remarks

In summary, MOFs have emerged as a highly promising class of porous materials for photocatalytic applications. Nevertheless, concerns arise regarding the release of toxic molecules from MOFs during photodegradation, emphasizing the need to develop environmentally benign and water-stable MOFs with high LD_{50} values for water desalination.

The reusability of MOFs and the minimization of other species' involvement, such as H_2O_2 or sulfate species, are critical for practical applications, especially in wastewater treatment plants. Engineering MOF-based photocatalysts necessitates careful consideration of various factors, including water composition, temperature, pH, the concentration of organic pollutants, long-term stability, and recyclability.

While the development of low-cost and highly durable MOF-based photocatalysts is still in its early stages, exploring innovative approaches such as increasing the pore size of POM-based architecture holds promise for enhancing stability and photocatalytic activity. However, challenges related to complex synthesis and low efficiency hinder the widespread application of these materials in photodegradation.

To overcome these challenges, incorporating POM-based materials supported by covalent bonds can enhance water stability while modifying organic linkers can improve visible light absorption properties of POMs and enhance the separation and reduction of photoinduced electron–hole pairs. The synergistic combination of POMs and MOFs represents a rare architecture with the potential for enhanced performance.

The prospects for MOF-based photocatalysts are promising but require further research and development to exploit their potential fully. Fabricating various POM-based materials with different combinations of metal–ligand systems will enhance photodegradation properties. Additionally, exploring the mechanisms associated with POM-based photocatalysts through applying hybrid functions, DFT, and ML techniques will contribute to a deeper understanding of their photocatalytic behavior.

Considering various aspects, such as different metal ions, cages, and organic ligands that influence light absorption, electron–hole pair separation, and charge transfer processes, is

crucial for advancing the design and optimization of MOF-based photocatalysts. Addressing the issue of POM leaching can be achieved by introducing organic and inorganic supports, which demand further attention from researchers.

Theoretical studies and tuning of these complex molecules for improved photocatalytic performance are ongoing. While DFT has been extensively utilized for such materials, the application of ML and hybrid functions for predicting the photocatalytic mechanisms of these photoactive materials is still at an early stage.

Overall, photoactive MOFs and their composites are promising as multifunctional water treatment and desalination materials. However, to fully harness their potential, it is essential to continue investing in comprehensive research and development efforts. By doing so, we can unlock the full capabilities of MOFs and pave the way for their practical implementation in addressing critical environmental challenges.

Abbreviations

2,5-H_2pdc	2,5 Pyridine dicarboxylic acid
2,6-pdc	2,6 Pyridine dicarboxylic acid
AOPs	Advanced oxidation processes
ATA	2-Aminoterephthalic acid
BDC	1,4-Benzenedicarboxylate
BDP	1,4-Benzenedipyrazolate
bio-MOF-11	Submicron-sized water-stable metal organic framework
bix	1,4′-Bis(imidazole-1-ylmethyl)benzene
bpy	4,4′ Bipyridine
btp	Bis(1,2,4- triazol-1-yl)hexane
BTP	1,3,5-Tris(1*H*-pyrazol-4-yl)benzene
CB	Conduction band
CP	Coordination polymer
CT	Charge transfer
CV	Crystal violet
dcbpyno	2,2′-Bipyridine-3,3′-dicarboxylate-1,1′-dioxide
DFT	Density functional theory
DOS	Density of state
dpa	1,2-Bis(4-pyridyl)-ethane
DRS	Differential reflectance spectroscopy
DTA	2,5-Di(1*H*-imidazole-1-yl)terephthalic acid
ESR	Electron spin resonance
HKUST-1	Hong Cong university of science and technology
HOCO	Highest occupied crystal orbitals
HSAB	Hard soft acid base
IPA	Isopropanol
IRMOF	Isoreticular MOF
KS-DFT	Kohn–Sham density functional theory
LD	Lethal dose
LMCT	Ligand to metal charge transfer
LUCO	Lowest unoccupied crystal orbitals
MB	Methylene blue
MIL	Matériaux de l'institut Lavoisier
ML	Machine learning
MMCT	Metal–metal charge transfer
MO	Methyl orange
MOF	Metal organic frameworks
MV	Methyl violet
PAH	Polyaromatic hydrocarbons
PANI	Polyaniline
PCN	Porus coordination network
p-DOS	Partial density of states
Phen	1,10-Phenanthroline
PL	Photoluminescence
POM	Polyoxometallates
PPCP	Pharmaceuticals and personal care product
PSM	Post synthetic modification
pzc	Pyrazinecarboxylate
QM	Quantum mechanical
Rh-B	Rhodamine B
ROS	Reactive oxygen species
SDCA	2,2′-Diamino-4,4′-stilbenedicarboxylic acid
SDWA	Safe drinking water act
TD-DFT	Time-dependent density functional theory
TEOA	Triethanolamine
UiO	Universitetet i Oslo
UNESCO	United nations educational, scientific and cultural organization
VB	Valence band
ZIF	Zeolitic imidazolate frameworks

Conflicts of interest

There are no conflicts to declare.

Acknowledgements

This work is supported by the Singapore Ministry of Education academic research grant Tier 2 (MOE-T2EP50121-0007) and 111 Project (D20015).

References

1 M. S. Khan, M. Khalid, M. Shahid, M. Shahid, M. Shahid and M. Shahid, What Triggers Dye Adsorption by Metal Organic Frameworks? The Current Perspectives, *Adv. Mater.*, 2020, **1**(6), 1575–1601, DOI: 10.1039/d0ma00291g.

2 M. Shirkhodaie, S. Seidi, F. Shemirani and F. Zaroudi, Environmental Contaminant Analysis: Concerns Inspiring the Emergence of MOF Composites, *TrAC, Trends Anal. Chem.*, 2023, **164**, 117109, DOI: 10.1016/j.trac.2023.117109.

3 K. K. Chenab, B. Sohrabi, A. Jafari and S. Ramakrishna, Water Treatment: Functional Nanomaterials and Applications from Adsorption to Photodegradation, *Mater. Today Chem.*, 2020, **16**, 100262, DOI: 10.1016/j.mtchem.2020.100262.

4 T. Meng, J. Zhang, H. Wang, N. Fu, M. Wang, W. Li, R. Shi, B. Peng, P. Li and Z. Deng, Multifunctional CuO-Coated Mesh for Wastewater Treatment: Effective Oil/Water Separation, Organic Contaminants Photodegradation, and Bacterial Photodynamic Inactivation, *Adv. Mater.*

Interfaces, 2021, **8**(22), 2101179, DOI: **10.1002/admi.202101179**.

5 Z. Zhang, Y. Zhong, W. Zhang, P. Zhao, H. Li and X. Liu, The Preparation and Application in Adsorptive Removal Hazardous Materials of MOF-Derived Materials, *J. Inorg. Organomet. Polym. Mater.*, 2023, DOI: **10.1007/s10904-023-02784-9**.

6 M. S. Ahmad, M. Khalid, M. Khalid, M. S. Khan, M. Shahid, M. Ali Shahid, M. Shahid, M. Shahid and M. Ahmad, Ni(II)-Based One Dimensional Coordination Polymers for Environmental Remediation: Design, Topology, Magnetism and the Selective Adsorption of Cationic Dyes, *CrystEngComm*, 2021, **23**(36), 6253–6266, DOI: **10.1039/d1ce00815c**.

7 M. S. Khan, M. A. H. Ansari, M. Khalid, M. Shahid and M. Ahmad, Synthesis, Characterization, Single-Crystal X-Ray Study and Sensing Properties of a Designed Dinuclear Cu(II) System, *Inorg. Nano-Met. Chem.*, 2023, 1–8, DOI: **10.1080/24701556.2023.2188454**.

8 O. US EPA, *Drinking Water Regulations*, **https://www.epa.gov/dwreginfo/drinking-water-regulations**, (accessed 2023-05-15).

9 S. Kamal, M. Khalid, M. Shahnawaz Khan and M. Shahid, Metal Organic Frameworks and Their Composites as Effective Tools for Sensing Environmental Hazards: An up to Date Tale of Mechanism, Current Trends and Future Prospects, *Coord. Chem. Rev.*, 2023, **474**, 214859, DOI: **10.1016/j.ccr.2022.214859**.

10 K.-G. Liu, F. Bigdeli, Z. Sharifzadeh, S. Gholizadeh and A. Morsali, Role of Metal–Organic Framework Composites in Removal of Inorganic Toxic Contaminants, *J. Cleaner Prod.*, 2023, **404**, 136709, DOI: **10.1016/j.jclepro.2023.136709**.

11 R. N. Amador, M. Carboni and D. Meyer, Sorption and Photodegradation under Visible Light Irradiation of an Organic Pollutant by a Heterogeneous UiO-67–Ru–Ti MOF Obtained by Post-Synthetic Exchange, *RSC Adv.*, 2017, **7**(1), 195–200, DOI: **10.1039/C6RA26552A**.

12 T. Jiang, B. Wang, B. Gao, N. Cheng, Q. Feng, M. Chen and S. Wang, Degradation of Organic Pollutants from Water by Biochar-Assisted Advanced Oxidation Processes: Mechanisms and Applications, *J. Hazard. Mater.*, 2023, **442**, 130075, DOI: **10.1016/j.jhazmat.2022.130075**.

13 T. H. Habtemariam, V. J. T. Raju and Y. Chebude, Pillared-Layer Metal–Organic Frameworks (MOFs) for Photodegradation of Methyl Orange in Wastewater, *Adv. Opt. Mater.*, 2023, **11**, 2202843, DOI: **10.1002/adom.202202843**.

14 M. S. Khan and M. Shahid, Improving water quality using metal–organic frameworks, in *Metal–Organic Frameworks for Environmental Remediation*, ACS Symposium Series; American Chemical Society, 2021, vol. 1395, pp. 171–191, DOI: DOI: **10.1021/bk-2021-1395.ch007**.

15 C. Yan, J. Jin, J. Wang, F. Zhang, Y. Tian, C. Liu, F. Zhang, L. Cao, Y. Zhou and Q. Han, Metal–Organic Frameworks (MOFs) for the Efficient Removal of Contaminants from Water: Underlying Mechanisms, Recent Advances, Challenges, and Future Prospects, *Coord. Chem. Rev.*, 2022, **468**, 214595, DOI: **10.1016/j.ccr.2022.214595**.

16 R. Song, J. Yao, M. Yang, Z. Ye, Z. Xie and X. Zeng, Active Site Regulated Z-Scheme MIL-101(Fe)/Bi_2WO_6/Fe(III) with the Synergy of Hydrogen Peroxide and Visible-Light-Driven Photo-Fenton Degradation of Organic Contaminants, *Nanoscale*, 2022, **14**(18), 7055–7074, DOI: **10.1039/D1NR07915H**.

17 Y. Zhang, Q. Niu, X. Gu, N. Yang and G. Zhao, Recent Progress on Carbon Nanomaterials for the Electrochemical Detection and Removal of Environmental Pollutants, *Nanoscale*, 2019, **11**(25), 11992–12014, DOI: **10.1039/C9NR02935D**.

18 R. Deka, V. Kumar, R. Rajak and S. M. Mobin, Two-Dimensional Layered Nickel-Based Coordination Polymer for Supercapacitive Performance, *Sustainable Energy Fuels*, 2022, **6**(12), 3014–3024, DOI: **10.1039/D2SE00527A**.

19 M. S. Khan, M. Khalid, M. Shahid, M. Shahid, M. Shahid and M. Shahid, A Co(II) Coordination Polymer Derived from Pentaerythritol as an Efficient Photocatalyst for the Degradation of Organic Dyes, *Polyhedron*, 2021, **196**, 114984, DOI: **10.1016/j.poly.2020.114984**.

20 K. Tanji, I. El Mrabet, Y. Fahoul, I. Jellal, M. Benjelloun, M. Belghiti, M. El Hajam, Y. Naciri, A. El Gaidoumi, B. El Bali, H. Zaitan and A. Kherbeche, Epigrammatic Progress on the Photocatalytic Properties of ZnO and TiO_2 Based Hydroxyapatite@photocatlyst toward Organic Molecules Photodegradation: A Review, *J. Water Process. Eng.*, 2023, **53**, 103682, DOI: **10.1016/j.jwpe.2023.103682**.

21 Y. Li, L. Liu, T. Meng, L. Wang and Z. Xie, Structural Engineering of Ionic MOF@COF Heterointerface for Exciton-Boosting Sunlight-Driven Photocatalytic Filter, *ACS Nano*, 2023, **17**(3), 2932–2942, DOI: **10.1021/acsnano.2c11339**.

22 A. Ahmed, A. Fatima, A. Fatima, S. Shakya, Q. Inamur Rahman, M. Ahmad, S. Javed, H. S. AlSalem and A. Ahmad, Crystal Structure, Topology, DFT and Hirshfeld Surface Analysis of a Novel Charge Transfer Complex (L3) of Anthraquinone and 4-{[(Anthracen-9-Yl)Meth-Yl] Amino}-Benzoic Acid (L2) Exhibiting Photocatalytic Properties: An Experimental and Theoretical Approach, *Molecules*, 2022, **27**(5), 1724, DOI: **10.3390/molecules27051724**.

23 M. S. Khan, M. Khalid, M. S. Ahmad, M. Shahid, M. Shahid, M. Shahid, M. Shahid and M. Ahmad, Catalytic Activity of Mn(III) and Co(III) Complexes: Evaluation of Catechol Oxidase Enzymatic and Photodegradation Properties, *Res. Chem. Intermed.*, 2020, **46**(6), 2985–3006, DOI: **10.1007/s11164-020-04127-6**.

24 *Novel Metal–Organic Framework Cocrystal Strategy for Significantly Enhancing Photocatalytic Performance – Liu – Advanced Functional Materials – Wiley Online Library*, **https://onlinelibrary.wiley.com/doi/full/10.1002/adfm.202306871**, (accessed 2023-09-12).

25 M. S. Refat, H. A. Saad, A. A. Gobouri, M. Alsawat, A. M. A. Adam, S. Shakya, A. Gaber, A. Gaber, A. M. A. Alsuhaibani, R. Z. Hamza and S. M. El-

Megharbel, Synthesis and Spectroscopic Characterizations of Nanostructured Charge Transfer Complexes Associated between Moxifloxacin Drug Donor and Metal Chloride Acceptors as a Catalytic Agent in a Recycling of Wastewater, *J. Mol. Liq.*, 2021, 118121, DOI: 10.1016/j.molliq.2021.118121.

26 M. Ahmad, J. Chen, J. Liu, Y. Zhang, Z. Song, S. Afzal, W. Raza, L. Zeb, A. Mehmood, A. Hussain, J. Zhang, X.-Z. Fu and J.-L. Luo, Metal–Organic Framework-Based Single-Atom Electro-/Photocatalysts: Synthesis, Energy Applications, and Opportunities, *Carbon Energy*, 2023, e382, DOI: 10.1002/cey2.382.

27 N. Celebi, M. Y. Aydin, F. Soysal, N. Yıldız and K. Salimi, Core/Shell PDA@UiO-66 Metal–Organic Framework Nanoparticles for Efficient Visible-Light Photodegradation of Organic Dyes, *ACS Appl. Nano Mater.*, 2020, **3**(11), 11543–11554, DOI: 10.1021/acsanm.0c02636.

28 O. M. Yaghi and H. Li, Hydrothermal Synthesis of a Metal–Organic Framework Containing Large Rectangular Channels, *J. Am. Chem. Soc.*, 1995, **117**(41), 10401–10402, DOI: 10.1021/ja00146a033.

29 M. Eddaoudi, D. B. Moler, H. Li, B. Chen, T. M. Reineke, M. O'Keeffe and O. M. Yaghi, Modular Chemistry: Secondary Building Units as a Basis for the Design of Highly Porous and Robust Metal–Organic Carboxylate Frameworks, *Acc. Chem. Res.*, 2001, **34**(4), 319–330, DOI: 10.1021/ar000034b.

30 R. Rajak, M. Saraf, P. Kumar, K. Natarajan and S. M. Mobin, Construction of a Cu-Based Metal–Organic Framework by Employing a Mixed-Ligand Strategy and Its Facile Conversion into Nanofibrous CuO for Electrochemical Energy Storage Applications, *Inorg. Chem.*, 2021, **60**(22), 16986–16995, DOI: 10.1021/acs.inorgchem.1c02062.

31 R. Rajak, M. Saraf, S. K. Verma, R. Kumar and S. M. Mobin, Dy(III)-Based Metal–Organic Framework as a Fluorescent Probe for Highly Selective Detection of Picric Acid in Aqueous Medium, *Inorg. Chem.*, 2019, **58**(23), 16065–16074, DOI: 10.1021/acs.inorgchem.9b02611.

32 J. He, Y. Zhang, J. He, X. Zeng, X. Hou and Z. Long, Enhancement of Photoredox Catalytic Properties of Porphyrinic Metal–Organic Frameworks Based on Titanium Incorporation via Post-Synthetic Modification, *Chem. Commun.*, 2018, **54**(62), 8610–8613, DOI: 10.1039/C8CC04891F.

33 Q. Wang, Q. Gao, A. M. Al-Enizi, A. Nafady and S. Ma, Recent Advances in MOF-Based Photocatalysis: Environmental Remediation under Visible Light, *Inorg. Chem. Front.*, 2020, **7**(2), 300–339, DOI: 10.1039/C9QI01120J.

34 S. Kampouri, F. M. Ebrahim, M. Fumanal, M. Nord, P. A. Schouwink, R. Elzein, R. Addou, G. S. Herman, B. Smit, C. P. Ireland and K. C. Stylianou, Enhanced Visible-Light-Driven Hydrogen Production through MOF/MOF Heterojunctions, *ACS Appl. Mater. Interfaces*, 2021, **13**(12), 14239–14247, DOI: 10.1021/acsami.0c23163.

35 H. Ramezanalizadeh and F. Manteghi, Synthesis of a Novel MOF/$CuWO_4$ Heterostructure for Efficient Photocatalytic Degradation and Removal of Water Pollutants, *J. Cleaner Prod.*, 2018, **172**, 2655–2666, DOI: 10.1016/j.jclepro.2017.11.145.

36 Q. Lai, X.-X. Li and S.-T. Zheng, All-Inorganic POM Cages and Their Assembly: A Review, *Coord. Chem. Rev.*, 2023, **482**, 215077, DOI: 10.1016/j.ccr.2023.215077.

37 X.-J. Dui, W.-B. Yang, X.-Y. Wu, X. Kuang, J.-Z. Liao, R. Yu and C.-Z. Lu, Two Novel POM-Based Inorganic–Organic Hybrid Compounds: Synthesis, Structures, Magnetic Properties, Photodegradation and Selective Absorption of Organic Dyes, *Dalton Trans.*, 2015, **44**(20), 9496–9505, DOI: 10.1039/C5DT01042J.

38 R. K. Das, J. P. Kar and S. Mohapatra, Enhanced Photodegradation of Organic Pollutants by Carbon Quantum Dot (CQD) Deposited Fe_3O_4@mTiO_2 Nano-Pom-Pom Balls, *Ind. Eng. Chem. Res.*, 2016, **55**(20), 5902–5910, DOI: 10.1021/acs.iecr.6b00792.

39 D.-Y. Zhou, G.-Y. Pan, M.-L. Xu, X. He, T. Li, F.-T. Liu, F.-H. Jiang and K. Li, Metal–Organic Framework-Derived Porous Carbon-Mediated ZnO–Nano-ZnO Core–Shell Structure with Excellent Photocatalytic Activity, *CrystEngComm*, 2023, **25**(3), 425–431, DOI: 10.1039/D2CE01476A.

40 L. Hu, J. Chen, Y. Wei, M. Wang, Y. Xu, C. Wang, P. Gao, Y. Liu, C. Liu, Y. Song, N. Ding, X. Liu and R. Wang, Photocatalytic Degradation Effect and Mechanism of Karenia Mikimotoi by Non-Noble Metal Modified TiO_2 Loading onto Copper Metal Organic Framework (SNP-TiO_2@Cu-MOF) under Visible Light, *J. Hazard. Mater.*, 2023, **442**, 130059, DOI: 10.1016/j.jhazmat.2022.130059.

41 Z. Durmus, R. Köferstein, T. Lindenberg, F. Lehmann, D. Hinderberger and A. W. Maijenburg, Preparation and Characterization of Ce-MOF/g-C_3N_4 Composites and Evaluation of Their Photocatalytic Performance, *Ceram. Int.*, 2023, **49**(14), 24428–24441, DOI: 10.1016/j.ceramint.2023.01.063.

42 J.-J. Jiang, F.-J. Zhang and Y.-R. Wang, Review of Different Series of MOF/g-C_3N_4 Composites for Photocatalytic Hydrogen Production and CO_2 Reduction, *New J. Chem.*, 2023, **47**(4), 1599–1609, DOI: 10.1039/D2NJ05260A.

43 M. S. Khan and M. Shahid, Chapter 2 – Synthesis of metal–organic frameworks (MOFs): routes to various MOF topologies, morphologies, and composites, in *Electrochemical Applications of Metal–Organic Frameworks*, ed. Dave S., Sahu R. and Tripathy B. C., Elsevier, 2022, pp. 17–35, DOI: DOI: 10.1016/B978-0-323-90784-2.00007-1.

44 S. Kamal, M. Khalid, M. S. Khan, M. Shahid and M. Ahmad, Amine- and Imine-Functionalized Mn-Based MOF as an Unusual Turn-On and Turn-Off Sensor for D10 Heavy Metal Ions and an Efficient Adsorbent to Capture Iodine, *Cryst. Growth Des.*, 2022, **22**(5), 3277–3294, DOI: 10.1021/acs.cgd.2c00092.

45 S. Kamal, M. Khalid, M. S. Khan, M. Shahid and M. Ahmad, A Zinc(II) MOF for Recognition of Nitroaromatic Explosive and Cr(III) Ion, *J. Solid State Chem.*, 2022, **315**, 123482, DOI: 10.1016/j.jssc.2022.123482.

46 K. Iman, M. N. Ahamad, Monika, A. Ansari, H. A. M. Saleh, M. S. Khan, M. Ahmad, R. A. Haque, M. Shahid, M. Shahid and M. Shahid, How to Identify a Smoker: A Salient Crystallographic Approach to Detect Thiocyanate Content, *RSC Adv.*, 2021, **11**(28), 16881–16891, DOI: **10.1039/d1ra01749g**.

47 W. Chaikittisilp, K. Ariga and Y. Yamauchi, A New Family of Carbon Materials: Synthesis of MOF-Derived Nanoporous Carbons and Their Promising Applications, *J. Mater. Chem. A*, 2013, **1**(1), 14–19, DOI: **10.1039/C2TA00278G**.

48 N. L. Rosi, J. Kim, M. Eddaoudi, B. Chen, M. O'Keeffe and O. M. Yaghi, Rod Packings and Metal–Organic Frameworks Constructed from Rod-Shaped Secondary Building Units, *J. Am. Chem. Soc.*, 2005, **127**(5), 1504–1518, DOI: **10.1021/ja045123o**.

49 M. N. Ahamad, M. S. Khan, M. Shahid, M. Shahid, M. Shahid, M. Shahid and M. Ahmad, Metal Organic Frameworks Decorated with Free Carboxylic Acid Groups: Topology, Metal Capture and Dye Adsorption Properties, *Dalton Trans.*, 2020, **49**(41), 14690–14705, DOI: **10.1039/d0dt02949a**.

50 S. Kamal, M. Khalid, M. S. Khan, M. Shahid and M. Ahmad, A Bifunctionalised Pb-Based MOF for Iodine Capture and Dyes Removal, *Dalton Trans.*, 2023, **52**(14), 4501–4516, DOI: **10.1039/D3DT00237C**.

51 Q. Deng, X. Liu, Z. Li, H. Fan, Y. Zhang and H. Y. Yang, Cobalt–Nickel Bimetallic Sulfide (NiS_2/CoS_2) Based Dual-Carbon Framework for Super Sodium Ion Storage, *J. Colloid Interface Sci.*, 2023, **633**, 480–488, DOI: **10.1016/j.jcis.2022.11.083**.

52 *Understanding the Highly Reversible Potassium Storage of Hollow Ternary (Bi–Sb)2S3@N-C Nanocube | ACS Nano*, **https://pubs.acs.org/doi/full/10.1021/acsnano.2c12703**, (accessed 2023-04-13).

53 D. Yan, H. Y. Yang and Y. Bai, Tactics to Optimize Conversion-Type Metal Fluoride/Sulfide/Oxide Cathodes toward Advanced Lithium Metal Batteries, *Nano Res.*, 2023, **16**, 8173–8190, DOI: **10.1007/s12274-023-5427-7**.

54 T. C. Li, Y. Lim, X. L. Li, S. Luo, C. Lin, D. Fang, S. Xia, Y. Wang and H. Y. Yang, A Universal Additive Strategy to Reshape Electrolyte Solvation Structure toward Reversible Zn Storage, *Adv. Energy Mater.*, 2022, **12**(15), 2103231, DOI: **10.1002/aenm.202103231**.

55 S. Huang, S. Huang, S. Huang, Z. Wang, Y. Von Lim, Y. Wang, Y. Wang, Y. Li, D. Zhang and H. Y. Yang, Recent Advances in Heterostructure Engineering for Lithium–Sulfur Batteries, *Adv. Energy Mater.*, 2021, **11**(10), 2003689, DOI: **10.1002/aenm.202003689**.

56 Y. Zhao, J. Zhang, Y. Xie, B. Sun, J. Jiang, J. Jiang, W.-J. Jiang, W.-J. Jiang, S. Xi, S. Xi, S. Xi, H. Y. Yang, K. Yan, S. Wang, X. Guo, P. Li, Z. J. Han, X. Lu, H. Liu and G. Wang, Constructing Atomic Heterometallic Sites in Ultrathin Nickel-Incorporated Cobalt Phosphide Nanosheets via a Boron-Assisted Strategy for Highly Efficient Water Splitting, *Nano Lett.*, 2021, **21**(1), 823–832, DOI: **10.1021/acs.nanolett.0c04569**.

57 Q. Wang, L. Cao, S.-J. Liang, W. Wu, W. Wu, G. Wang, C. H. Lee, W. L. Ong, W.-L. Ong, H. Y. Yang, L. K. Ang, S. A. Yang and Y. S. Ang, Efficient Ohmic Contacts and Built-in Atomic Sublayer Protection in $MoSi_2N_4$ and WSi_2N_4 Monolayers, *npj 2D Mater. Appl.*, 2021, **5**(1), 1–9, DOI: **10.1038/s41699-021-00251-y**.

58 M. S. Khan, M. Khalid, M. S. Ahmad, S. Kamal, M. Shahid, M. Shahid, M. Shahid, M. Shahid and M. Ahmad, Effect of Structural Variation on Enzymatic Activity in Tetranuclear (Cu_4) Clusters with Defective Cubane Core, *J. Biomol. Struct. Dyn.*, 2021, 1–14, DOI: **10.1080/07391102.2021.1924263**.

59 M. S. Khan, M. U. Hayat, M. Khanam, H. Saeed, M. Owais, M. Khalid, M. Shahid, M. Shahid, M. Shahid, M. Shahid and M. Ahmad, Role of Biologically Important Imidazole Moiety on the Antimicrobial and Anticancer Activity of Fe(III) and Mn(II) Complexes, *J. Biomol. Struct. Dyn.*, 2020, **39**(11), 4037–4050, DOI: **10.1080/07391102.2020.1776156**.

60 M. S. Khan, Z. Y. Leong, D.-S. Li, J. Qiu, X. Xu and H. Y. Yang, A Mini Review on Metal–Organic Framework-Based Electrode Materials for Capacitive Deionization, *Nanoscale*, 2023, **15**, 15929–15949, DOI: **10.1039/D3NR03993E**.

61 R. Ettlinger, U. Lächelt, R. Gref, P. Horcajada, T. Lammers, C. Serre, P. Couvreur, R. E. Morris and S. Wuttke, Toxicity of Metal–Organic Framework Nanoparticles: From Essential Analyses to Potential Applications, *Chem. Soc. Rev.*, 2022, **51**(2), 464–484, DOI: **10.1039/D1CS00918D**.

62 M. Ding, X. Cai and H.-L. Jiang, Improving MOF Stability: Approaches and Applications, *Chem. Sci.*, 2019, **10**(44), 10209–10230, DOI: **10.1039/C9SC03916C**.

63 S. Fajal, A. Hassan, W. Mandal, M. M. Shirolkar, S. Let, N. Das and S. K. Ghosh, Ordered Macro/Microporous Ionic Organic Framework for Efficient Separation of Toxic Pollutants from Water, *Angew. Chem.*, 2023, **135**(1), e202214095, DOI: **10.1002/ange.202214095**.

64 S. Fajal, W. Mandal, S. Mollick, Y. D. More, A. Torris, S. Saurabh, M. M. Shirolkar and S. K. Ghosh, Berichtigung: Trap Inlaid Cationic Hybrid Composite Material for Efficient Segregation of Toxic Chemicals from Water, *Angew. Chem.*, 2022, **134**(43), e202212921, DOI: **10.1002/ange.202212921**.

65 W. Mandal, S. Fajal, P. Samanta, S. Dutta, M. M. Shirolkar, Y. D. More and S. K. Ghosh, Selective and Sensitive Recognition of Specific Types of Toxic Organic Pollutants with a Chemically Stable Highly Luminescent Porous Organic Polymer (POP), *ACS Appl. Polym. Mater.*, 2022, **4**(11), 8633–8644, DOI: **10.1021/acsapm.2c01538**.

66 I. M. Khan, A. Khan, S. Shakya and M. Islam, Exploring the Photocatalytic Activity of Synthesized Hydrogen Bonded Charge Transfer Co-Crystal of Chloranilic Acid with 2-Ethylimidazole: DFT, Molecular Docking and Spectrophotometric Studies in Different Solvents, *J. Mol. Struct.*, 2023, **1277**, 134862, DOI: **10.1016/j.molstruc.2022.134862**.

67 Y. Li, H. Xu, S. Ouyang and J. Ye, Metal–Organic Frameworks for Photocatalysis, *Phys. Chem. Chem. Phys.*, 2016, **18**(11), 7563–7572, DOI: **10.1039/C5CP05885F**.

68 J. Qiu, X. Zhang, Y. Feng, X. Zhang, H. Wang and J. Yao, Modified Metal–Organic Frameworks as Photocatalysts, *Appl. Catal., B*, 2018, **231**, 317–342, DOI: **10.1016/j.apcatb.2018.03.039**.

69 J. Bedia, V. Muelas-Ramos, M. Peñas-Garzón, A. Gómez-Avilés, J. J. Rodríguez and C. Belver, A Review on the Synthesis and Characterization of Metal Organic Frameworks for Photocatalytic Water Purification, *Catalysts*, 2019, **9**(1), 52, DOI: **10.3390/catal9010052**.

70 *Iron-Based Metal–Organic Frameworks (MOFs) for Visible-Light-Induced Photocatalysis | SpringerLink*, **https://link.springer.com/article/10.1007/s11164-017-3042-0**, (accessed 2023-05-15).

71 C.-X. Chen, Y.-Y. Xiong, X. Zhong, P. C. Lan, Z.-W. Wei, H. Pan, P.-Y. Su, Y. Song, Y.-F. Chen, A. Nafady, Sirajuddin and S. Ma, Enhancing Photocatalytic Hydrogen Production via the Construction of Robust Multivariate Ti-MOF/COF Composites, *Angew. Chem., Int. Ed.*, 2022, **61**(3), e202114071, DOI: **10.1002/anie.202114071**.

72 Y. Bai, S. Zhang, S. Feng, M. Zhu and S. Ma, The First Ternary Nd-MOF/GO/Fe_3O_4 Nanocomposite Exhibiting an Excellent Photocatalytic Performance for Dye Degradation, *Dalton Trans.*, 2020, **49**(31), 10745–10754, DOI: **10.1039/D0DT01648A**.

73 Q. Wang, G. Yang, Y. Fu, N. Li, D. Hao and S. Ma, Nanospace Engineering of Metal–Organic Frameworks for Heterogeneous Catalysis, *ChemNanoMat*, 2022, **8**(1), e202100396, DOI: **10.1002/cnma.202100396**.

74 N. A. Nordin, M. A. Mohammed, M. N. I. Salehmin and S. F. Mohd Yusoff, Photocatalytic Active Metal–Organic Framework and Its Derivatives for Solar-Driven Environmental Remediation and Renewable Energy, *Coord. Chem. Rev.*, 2022, **468**, 214639, DOI: **10.1016/j.ccr.2022.214639**.

75 Y. Liu, C. Tang, M. Cheng, M. Chen, S. Chen, L. Lei, Y. Chen, H. Yi, Y. Fu and L. Li, Polyoxometalate@Metal–Organic Framework Composites as Effective Photocatalysts, *ACS Catal.*, 2021, **11**(21), 13374–13396, DOI: **10.1021/acscatal.1c03866**.

76 H. Li, D. Li, M. Long, X. Bai, Q. Wen and F. Song, Solvothermal Synthesis of MIL-53Fe@g-C_3N_4 for Peroxymonosulfate Activation towards Enhanced Photocatalytic Performance, *Colloids Surf., A*, 2023, **658**, 130646, DOI: **10.1016/j.colsurfa.2022.130646**.

77 M. Yang, G. Ma, H. Yang, Z. Xiaoqiang, W. Yang and H. Hou, Advanced Strategies for Promoting the Photocatalytic Performance of $FeVO_4$ Based Photocatalysts: A Review of Recent Progress, *J. Alloys Compd.*, 2023, **941**, 168995, DOI: **10.1016/j.jallcom.2023.168995**.

78 W. Shi, X. Liu, T. Deng, S. Huang, M. Ding, X. Miao, C. Zhu, C. Zhu, Y. Zhu, W. Liu, F. Wu, C. Gao, C. Gao, S.-W. Yang, H. Y. Yang, J. Shen and X. Cao, Enabling Superior Sodium Capture for Efficient Water Desalination by a Tubular Polyaniline Decorated with Prussian Blue Nanocrystals, *Adv. Mater.*, 2020, **32**(33), 1907404, DOI: **10.1002/adma.201907404**.

79 Z. Yi Leong, Z. Y. Leong and H. Y. Yang, A Study of MnO_2 with Different Crystalline Forms for Pseudocapacitive Desalination, *ACS Appl. Mater. Interfaces*, 2019, **11**(14), 13176–13184, DOI: **10.1021/acsami.8b20880**.

80 F. Chen, Y. Huang, L. Guo, L. Sun, Y. Wang and H. Ying Yang, Dual-Ions Electrochemical Deionization: A Desalination Generator, *Energy Environ. Sci.*, 2017, **10**(10), 2081–2089, DOI: **10.1039/C7EE00855D**.

81 F. Chen, Y. Huang, Y. Huang, L. Guo, M. Ding and H. Y. Yang, A Dual-Ion Electrochemistry Deionization System Based on AgCl-$Na_{0.44}MnO_2$ Electrodes, *Nanoscale*, 2017, **9**(28), 10101–10108, DOI: **10.1039/c7nr01861d**.

82 M. Ding, W. Shi, L. Guo, Z. Y. Leong, A. Baji and H. Y. Yang, Bimetallic Metal–Organic Framework Derived Porous Carbon Nanostructures for High Performance Membrane Capacitive Desalination, *J. Mater. Chem.*, 2017, **5**(13), 6113–6121, DOI: **10.1039/c7ta00339k**.

83 M. Ding, K. K. R. Bannuru, Y. Wang, L. Guo, A. Baji and H. Y. Yang, Free-Standing Electrodes Derived from Metal–Organic Frameworks/Nanofibers Hybrids for Membrane Capacitive Deionization, *Adv. Mater. Technol.*, 2018, **3**(11), 1800135, DOI: **10.1002/admt.201800135**.

84 X. Huang and X. Liu, Strategies for Enhancing Hole Utilization on Organic-POM Hybrid Materials and Photocatalytic Degradation of Neonicotinoid Insecticides, *J. Photochem. Photobiol., A*, 2023, **435**, 114299, DOI: **10.1016/j.jphotochem.2022.114299**.

85 A. Gogoi, P. Mazumder, V. K. Tyagi, G. G. Tushara Chaminda, A. K. An and M. Kumar, Occurrence and Fate of Emerging Contaminants in Water Environment: A Review, *Groundw. Sustain. Dev.*, 2018, **6**, 169–180, DOI: **10.1016/j.gsd.2017.12.009**.

86 D. Awfa, M. Ateia, M. Fujii, M. S. Johnson and C. Yoshimura, Photodegradation of Pharmaceuticals and Personal Care Products in Water Treatment Using Carbonaceous-TiO_2 Composites: A Critical Review of Recent Literature, *Water Res.*, 2018, **142**, 26–45, DOI: **10.1016/j.watres.2018.05.036**.

87 U. Alam, Role of heterogeneous semiconductor photocatalysts in green organic synthesis, in *Photocatalysis for Environmental Remediation and Energy Production: Recent Advances and Applications*, ed. Garg S. and Chandra A., Springer International Publishing, Cham, 2023, Green Chemistry and Sustainable Technology, pp. 263–290, DOI: DOI: **10.1007/978-3-031-27707-8_11**.

88 A. Singh, U. Alam, P. Chakraborty, B. Sundararaju and N. Verma, A Sustainable Approach for the Production of Formate from CO_2 Using Microalgae as a Clean Biomass and Improvement Using Potassium-Doped g-C_3N_4, *Chem. Eng. J.*, 2023, **454**, 140303, DOI: **10.1016/j.cej.2022.140303**.

89 M. S. Khan, M. Khalid, M. S. Ahmad, M. Shahid, M. Shahid, M. Shahid, M. Shahid, M. Shahid and M. Ahmad, Three-in-One Is Really Better: Exploring the Sensing and Adsorption

Properties in a Newly Designed Metal–Organic System Incorporating a Copper(II) Ion, *Dalton Trans.*, 2019, **48**(34), 12918–12932, DOI: 10.1039/c9dt02578b.

90 C. Wang, X. Liu, N. K. Demir, J. Paul Chen and K. Li, Applications of Water Stable Metal–Organic Frameworks, *Chem. Soc. Rev.*, 2016, **45**(18), 5107–5134, DOI: 10.1039/C6CS00362A.

91 Q. Sun, L. Qin, C. Lai, S. Liu, W. Chen, F. Xu, D. Ma, Y. Li, S. Qian, Z. Chen, W. Chen and H. Ye, Constructing Functional Metal–Organic Frameworks by Ligand Design for Environmental Applications, *J. Hazard. Mater.*, 2023, **447**, 130848, DOI: 10.1016/j.jhazmat.2023.130848.

92 E. Haque, J. W. Jun and S. H. Jhung, Adsorptive Removal of Methyl Orange and Methylene Blue from Aqueous Solution with a Metal–Organic Framework Material, Iron Terephthalate (MOF-235), *J. Hazard. Mater.*, 2011, **185**(1), 507–511, DOI: 10.1016/j.jhazmat.2010.09.035.

93 G. An, W. Ma, Z. Sun, Z. Liu, B. Han, S. Miao, Z. Miao and K. Ding, Preparation of Titania/Carbon Nanotube Composites Using Supercritical Ethanol and Their Photocatalytic Activity for Phenol Degradation under Visible Light Irradiation, *Carbon*, 2007, **45**(9), 1795–1801, DOI: 10.1016/j.carbon.2007.04.034.

94 R. Andreozzi, V. Caprio, A. Insola and R. Marotta, Advanced Oxidation Processes (AOP) for Water Purification and Recovery, *Catal. Today*, 1999, **53**(1), 51–59, DOI: 10.1016/S0920-5861(99)00102-9.

95 É. Whelan, F. W. Steuber, T. Gunnlaugsson and W. Schmitt, Tuning Photoactive Metal–Organic Frameworks for Luminescence and Photocatalytic Applications, *Coord. Chem. Rev.*, 2021, **437**, 213757, DOI: 10.1016/j.ccr.2020.213757.

96 C. Brahmi, M. Benltifa, M. Ghali, F. Dumur, C. Simonnet-Jégat, V. Monnier, F. Morlet-Savary, L. Bousselmi and J. Lalevée, Polyoxometalates/Polymer Composites for the Photodegradation of Bisphenol-A, *J. Appl. Polym. Sci.*, 2021, **138**(34), 50864, DOI: 10.1002/app.50864.

97 H. Rezaei Ghalebi, S. Aber and A. Karimi, Keggin Type of Cesium Phosphomolybdate Synthesized via Solid-State Reaction as an Efficient Catalyst for the Photodegradation of a Dye Pollutant in Aqueous Phase, *J. Mol. Catal. A: Chem.*, 2016, **415**, 96–103, DOI: 10.1016/j.molcata.2016.01.031.

98 M. Liu, X.-F. Yang, H.-B. Zhu, B.-S. Di and Y. Zhao, A Robust Polyoxometalate-Templated Four-Fold Interpenetrating Metal–Organic Framework Showing Efficient Organic Dye Photodegradation in Various pH Aqueous Solutions, *Dalton Trans.*, 2018, **47**(15), 5245–5251, DOI: 10.1039/C8DT00366A.

99 Z. Abbas, N. Hussain, I. Ahmed and S. M. Mobin, Cu–Metal Organic Framework Derived Multilevel Hierarchy (Cu/Cu*x*O@NC) as a Bifunctional Electrode for High-Performance Supercapacitors and Oxygen Evolution Reaction, *Inorg. Chem.*, 2023, **62**(23), 8835–8845, DOI: 10.1021/acs.inorgchem.3c00308.

100 P. Kumar, N. Kaur, P. Tiwari, A. K. Gupta and S. M. Mobin, Gelatin-Coated Copper-Based Metal–Organic Framework for Controlled Insulin Delivery: Possibility toward Oral Delivery System, *ACS Mater. Lett.*, 2023, **5**(4), 1100–1108, DOI: 10.1021/acsmaterialslett.2c01175.

101 L. Jiang, Y. Dong, Y. Yuan, X. Zhou, Y. Liu and X. Meng, Recent Advances of Metal–Organic Frameworks in Corrosion Protection: From Synthesis to Applications, *Chem. Eng. J.*, 2022, **430**, 132823, DOI: 10.1016/j.cej.2021.132823.

102 S. A. Younis, E. E. Kwon, M. Qasim, K.-H. Kim, T. Kim, D. Kukkar, X. Dou and I. Ali, Metal–Organic Framework as a Photocatalyst: Progress in Modulation Strategies and Environmental/Energy Applications, *Prog. Energy Combust. Sci.*, 2020, **81**, 100870, DOI: 10.1016/j.pecs.2020.100870.

103 J.-Q. Liu, J. Chen, C. Fan, D. Luo, J. Huang, J. Ouyang, A. Nezamzadeh-Ejhieh, Y. Peng and M. Shahnawaz Khan, Recent Advances in Ti-Based MOFs in the Biomedical Applications, *Dalton Trans.*, 2022, **51**, 14817–14832, DOI: 10.1039/d2dt02470e.

104 W. Zhang, G. Ye, D. O. Liao, X. Chen, C. Lu, A. Nezamzadeh-Ejhieh, M. S. Khan, J.-Q. Liu, Y. Pan and D. Zhong, Recent Advances of Silver-Based Coordination Polymers on Antibacterial Applications, *Molecules*, 2022, **27**(21), 7166, DOI: 10.3390/molecules27217166.

105 L. Figueroa-Quintero, D. Villalgordo-Hernández, J. J. Delgado-Marín, J. Narciso, V. K. Velisoju, P. Castaño, J. Gascón and E. V. Ramos-Fernández, Post-Synthetic Surface Modification of Metal–Organic Frameworks and Their Potential Applications, *Small Methods*, 2023, **7**(4), 2201413, DOI: 10.1002/smtd.202201413.

106 Y. Zeng, G. Xu, X. Kong, G. Ye, J. Guo, C. Lu, A. Nezamzadeh-Ejhieh, M. Shahnawaz Khan, J. Liu and Y. Peng, Recent Advances of the Core–Shell MOFs in Tumour Therapy, *Int. J. Pharm.*, 2022, **627**, 122228, DOI: 10.1016/j.ijpharm.2022.122228.

107 W. Mandal, D. Majumder, S. Fajal, S. Let, M. M. Shirolkar and S. K. Ghosh, Post Engineering of a Chemically Stable MOF for Selective and Sensitive Sensing of Nitric Oxide, *Mol. Syst. Des. Eng.*, 2023, **8**, 756–766, DOI: 10.1039/D2ME00278G.

108 Y. Shi, Y. Zou, M. Zhang, M. Shahnawaz Khan, J. Yan, X. Zheng, W. Wang and Z. Xie, Metal–Organic Framework-Derived Photoelectrochemical Sensor: Structural Design and Biosensing Technology, *J. Mater. Chem. C*, 2023, **11**, 3692–3709, DOI: 10.1039/D2TC05338A.

109 S. Jiang, X. L. Li, D. Fang, W. Y. Lieu, C. Chen, M. S. Khan, D.-S. Li, B. Tian, Y. Shi and H. Y. Yang, Metal–Organic-Framework-Derived 3D Hierarchical Matrixes for High-Performance Flexible Li–S Batteries, *ACS Appl. Mater. Interfaces*, 2023, **15**(16), 20064–20074, DOI: 10.1021/acsami.2c22999.

110 Y. Zhao, Y. Zhang, X. Cao, J. Li and X. Hou, Synthesis of MOF on MOF Photocatalysts Using PCN-134 as Seed through Epitaxial Growth Strategy towards Nizatidine Degradation, *Chem. Eng. J.*, 2023, **465**, 143000, DOI: 10.1016/j.cej.2023.143000.

111 C. Du, Z. Zhang, G. Yu, H. Wu, H. Chen, L. Zhou, Y. Zhang, Y. Su, S. Tan, L. Yang, J. Song and S. Wang, A Review of

Metal Organic Framework (MOFs)-Based Materials for Antibiotics Removal via Adsorption and Photocatalysis, *Chemosphere*, 2021, **272**, 129501, DOI: 10.1016/j.chemosphere.2020.129501.

112 Ch. V. Reddy, K. R. Reddy, V. V. N. Harish, J. Shim, M. V. Shankar, N. P. Shetti and T. M. Aminabhavi, Metal–Organic Frameworks (MOFs)-Based Efficient Heterogeneous Photocatalysts: Synthesis, Properties and Its Applications in Photocatalytic Hydrogen Generation, CO_2 Reduction and Photodegradation of Organic Dyes, *Int. J. Hydrogen Energy*, 2020, **45**(13), 7656–7679, DOI: 10.1016/j.ijhydene.2019.02.144.

113 S. Kamal, M. Khalid, M. S. Khan, M. Shahid, M. Shahid, M. Shahid, M. Shahid, M. Ashafaq, I. Mantasha, M. S. Ahmad, M. Ahmad, M. Faizan, M. Faizan, M. Faizan and S. Ahmad, Synthesis, Characterization and DFT Studies of Water Stable Cd(II) Metal–Organic Clusters with Better Adsorption Property towards the Organic Pollutant in Waste Water, *Inorg. Chim. Acta*, 2020, **512**, 119872, DOI: 10.1016/j.ica.2020.119872.

114 J.-W. Yan, J. Wu, L. Lu, J. Wang, J. Guo, H. Sakiyama, M. Muddassir and M. Shahnawaz Khan, Photocatalytic Performances and Mechanisms of Two Coordination Polymers Based on Rigid Tricarboxylate, *J. Solid State Chem.*, 2022, 123602, DOI: 10.1016/j.jssc.2022.123602.

115 H. Zhang, G. Chen and D. W. Bahnemann, Photoelectrocatalytic Materials for Environmental Applications, *J. Mater. Chem.*, 2009, **19**(29), 5089–5121, DOI: 10.1039/B821991E.

116 *Understanding TiO_2 Photocatalysis: Mechanisms and Materials | Chemical Reviews*, https://pubs.acs.org/doi/full/10.1021/cr5001892, (accessed 2023-05-15).

117 N. Y. Donkadokula, A. K. Kola, I. Naz and D. Saroj, A Review on Advanced Physico-Chemical and Biological Textile Dye Wastewater Treatment Techniques, *Rev. Environ. Sci. Biotechnol.*, 2020, **19**(3), 543–560, DOI: 10.1007/s11157-020-09543-z.

118 X. Dong, Y. Li, D. Li, D. Liao, T. Qin, O. Prakash, A. Kumar and J. Liu, A New 3D 8-Connected Cd(II) MOF as a Potent Photocatalyst for Oxytetracycline Antibiotic Degradation, *CrystEngComm*, 2022, **24**(39), 6933–6943, DOI: 10.1039/D2CE01121B.

119 A. Singh, A. Kumar Singh, J. Liu and A. Kumar, Syntheses, Design Strategies, and Photocatalytic Charge Dynamics of Metal–Organic Frameworks (MOFs): A Catalyzed Photo-Degradation Approach towards Organic Dyes, *Catal. Sci. Technol.*, 2021, **11**(12), 3946–3989, DOI: 10.1039/D0CY02275F.

120 K. Iman, M. Shahid, M. Shahid, M. Shahid, M. Shahid, M. S. Khan, M. Ahmad and F. Sama, Topology, Magnetism and Dye Adsorption Properties of Metal Organic Frameworks (MOFs) Synthesized from Bench Chemicals, *CrystEngComm*, 2019, **21**(35), 5299–5309, DOI: 10.1039/c9ce01041f.

121 M. Singh and S. Neogi, Selective and Multicyclic CO_2 Adsorption with Visible Light-Driven Photodegradation of Organic Dyes in a Robust Metal–Organic Framework Embracing Heteroatom-Affixed Pores, *Inorg. Chem.*, 2022, **61**(28), 10731–10742, DOI: 10.1021/acs.inorgchem.2c00950.

122 P. Rassu, X. Ma and B. Wang, Engineering of Catalytically Active Sites in Photoactive Metal–Organic Frameworks, *Coord. Chem. Rev.*, 2022, **465**, 214561, DOI: 10.1016/j.ccr.2022.214561.

123 Z. Hasan and S. H. Jhung, Removal of Hazardous Organics from Water Using Metal–Organic Frameworks (MOFs): Plausible Mechanisms for Selective Adsorptions, *J. Hazard. Mater.*, 2015, **283**, 329–339, DOI: 10.1016/j.jhazmat.2014.09.046.

124 S. Sağlam, F. N. Türk and H. Arslanoğlu, Use and Applications of Metal–Organic Frameworks (MOF) in Dye Adsorption: Review, *J. Environ. Chem. Eng.*, 2023, **11**(5), 110568, DOI: 10.1016/j.jece.2023.110568.

125 M. S. Khan, M. Khalid, M. Shahid, M. Shahid, M. Shahid and M. Shahid, Engineered Fe_3 Triangle for the Rapid and Selective Removal of Aromatic Cationic Pollutants: Complexity Is Not a Necessity, *RSC Adv.*, 2021, **11**(5), 2630–2642, DOI: 10.1039/d0ra09586a.

126 M. M. Aljohani, S. D. Al-Qahtani, M. Alshareef, M. G. El-Desouky, A. A. El-Bindary, N. M. El-Metwaly and M. A. El-Bindary, Highly Efficient Adsorption and Removal Bio-Staining Dye from Industrial Wastewater onto Mesoporous Ag-MOFs, *Process Saf. Environ. Prot.*, 2023, **172**, 395–407, DOI: 10.1016/j.psep.2023.02.036.

127 N. Hu, J. Yu, L. Hou, C. Shi, K. Li, F. Hang and C. Xie, Amine-Functionalized MOF-Derived Carbon Materials for Efficient Removal of Congo Red Dye from Aqueous Solutions: Simulation and Adsorption Studies, *RSC Adv.*, 2023, **13**(1), 1–13, DOI: 10.1039/D2RA06513D.

128 K. M. V. Nguyen, A. V. N. Phan, N. T. Dang, T. Q. Tran, K. H. Duong, H. N. Nguyen and M. V. Nguyen, Efficiently Improving the Adsorption Capacity of the Rhodamine B Dye in a SO_3 H-Functionalized Chromium-Based Metal–Organic Framework, *Adv. Mater.*, 2023, **4**(12), 2636–2647, DOI: 10.1039/D3MA00123G.

129 X. Xin, Y. Jing, P. Li, X. Zhang, J. Li, L. Li and L. Zhang, Imidazole-Based Metal–Organic Framework for the "On 1–Off–On 2" Fluorescence-Based Detection of Picric Acid and the Adsorption of Congo Red, *Cryst. Growth Des.*, 2023, **23**(6), 3988–3995, DOI: 10.1021/acs.cgd.2c01186.

130 B. Lalchawimawia, A. Sil, T. Banerjee, N. Singh, A. Bhatnagar, R. Mukhopadhyay and A. Mandal, Metal–Organic Framework-Pesticide Interactions in Water: Present and Future Perspectives on Monitoring, Remediation and Molecular Simulation, *Coord. Chem. Rev.*, 2023, **490**, 215214, DOI: 10.1016/j.ccr.2023.215214.

131 S.-Y. Lee and S.-J. Park, TiO_2 Photocatalyst for Water Treatment Applications, *J. Ind. Eng. Chem.*, 2013, **19**(6), 1761–1769, DOI: 10.1016/j.jiec.2013.07.012.

132 Y. Li, H. Dong, L. Li, L. Tang, R. Tian, R. Li, J. Chen, Q. Xie, Z. Jin, J. Xiao, S. Xiao and G. Zeng, Recent Advances in Waste Water Treatment through Transition Metal Sulfides-Based Advanced Oxidation Processes, *Water Res.*, 2021, **192**, 116850, DOI: 10.1016/j.watres.2021.116850.

133 S. Yuan, L. Feng, K. Wang, J. Pang, M. Bosch, C. Lollar, Y. Sun, J. Qin, X. Yang, P. Zhang, Q. Wang, L. Zou, Y. Zhang, L. Zhang, Y. Fang, J. Li and H.-C. Zhou, Stable Metal–Organic Frameworks: Design, Synthesis, and Applications, *Adv. Mater.*, 2018, **30**(37), 1704303, DOI: **10.1002/adma.201704303**.

134 Y. Qin, M. Hao, D. Wang and Z. Li, Post-Synthetic Modifications (PSM) on Metal–Organic Frameworks (MOFs) for Visible-Light-Initiated Photocatalysis, *Dalton Trans.*, 2021, **50**(38), 13201–13215, DOI: **10.1039/D1DT02424H**.

135 *Engineering of Band Gap in Metal–Organic Frameworks by Functionalizing Organic Linker: A Systematic Density Functional Theory Investigation | The Journal of Physical Chemistry C*, **https://pubs.acs.org/doi/full/10.1021/jp405997r**, (accessed 2023-05-16).

136 T. Zhang, Y. Jin, Y. Shi, M. Li, J. Li and C. Duan, Modulating Photoelectronic Performance of Metal–Organic Frameworks for Premium Photocatalysis, *Coord. Chem. Rev.*, 2019, **380**, 201–229, DOI: **10.1016/j.ccr.2018.10.001**.

137 P. Sippel, D. Denysenko, A. Loidl, P. Lunkenheimer, G. Sastre and D. Volkmer, Dielectric Relaxation Processes, Electronic Structure, and Band Gap Engineering of MFU-4-Type Metal–Organic Frameworks: Towards a Rational Design of Semiconducting Microporous Materials, *Adv. Funct. Mater.*, 2014, **24**(25), 3885–3896, DOI: **10.1002/adfm.201400083**.

138 M. E. Foster, J. D. Azoulay, B. M. Wong and M. D. Allendorf, Novel Metal–Organic Framework Linkers for Light Harvesting Applications, *Chem. Sci.*, 2014, **5**(5), 2081–2090, DOI: **10.1039/C4SC00333K**.

139 M. A. Syzgantseva, C. P. Ireland, F. M. Ebrahim, B. Smit and O. A. Syzgantseva, Metal substitution as the method of modifying electronic structure of metal–organic frameworks, *J. Am. Chem. Soc.*, 2019, **141**(15), 6271–6278, DOI: **10.1021/jacs.8b13667**.

140 L. Shen, W. Wu, R. Liang, R. Lin and L. Wu, Highly Dispersed Palladium Nanoparticles Anchored on UiO-66(NH_2) Metal–Organic Framework as a Reusable and Dual Functional Visible-Light-Driven Photocatalyst, *Nanoscale*, 2013, **5**(19), 9374–9382, DOI: **10.1039/C3NR03153E**.

141 R. Kitaura, K. Seki, G. Akiyama and S. Kitagawa, Porous Coordination-Polymer Crystals with Gated Channels Specific for Supercritical Gases, *Angew. Chem., Int. Ed.*, 2003, **42**(4), 428–431, DOI: **10.1002/anie.200390130**.

142 T. Zhang and W. Lin, Metal–Organic Frameworks for Artificial Photosynthesis and Photocatalysis, *Chem. Soc. Rev.*, 2014, **43**(16), 5982–5993, DOI: **10.1039/C4CS00103F**.

143 S. Bordiga, C. Lamberti, G. Ricchiardi, L. Regli, F. Bonino, A. Damin, K.-P. Lillerud, M. Bjorgen and A. Zecchina, Electronic and Vibrational Properties of a MOF-5 Metal–Organic Framework: ZnO Quantum Dot Behaviour, *Chem. Commun.*, 2004, (20), 2300–2301, DOI: **10.1039/B407246D**.

144 M. Alvaro, E. Carbonell, B. Ferrer, F. X. Llabrés i Xamena and H. Garcia, Semiconductor Behavior of a Metal–Organic Framework (MOF), *Chem.–Eur. J.*, 2007, **13**(18), 5106–5112, DOI: **10.1002/chem.200601003**.

145 H. Sepehrmansourie, H. Alamgholiloo, N. Noroozi Pesyan and M. A. Zolfigol, A MOF-on-MOF Strategy to Construct Double Z-Scheme Heterojunction for High-Performance Photocatalytic Degradation, *Appl. Catal., B*, 2023, **321**, 122082, DOI: **10.1016/j.apcatb.2022.122082**.

146 *A New Zirconium Inorganic Building Brick Forming Metal Organic Frameworks with Exceptional Stability | Journal of the American Chemical Society*, **https://pubs.acs.org/doi/full/10.1021/ja8057953**, (accessed 2023-05-16).

147 Y. Fu, D. Sun, Y. Chen, R. Huang, Z. Ding, X. Fu and Z. Li, An Amine-Functionalized Titanium Metal–Organic Framework Photocatalyst with Visible-Light-Induced Activity for CO_2 Reduction, *Angew. Chem., Int. Ed.*, 2012, **51**(14), 3364–3367, DOI: **10.1002/anie.201108357**.

148 J. Joseph, S. Iftekhar, V. Srivastava, Z. Fallah, E. N. Zare and M. Sillanpää, Iron-Based Metal–Organic Framework: Synthesis, Structure and Current Technologies for Water Reclamation with Deep Insight into Framework Integrity, *Chemosphere*, 2021, **284**, 131171, DOI: **10.1016/j.chemosphere.2021.131171**.

149 X. Li, W. Guo, Z. Liu, R. Wang and H. Liu, Fe-Based MOFs for Efficient Adsorption and Degradation of Acid Orange 7 in Aqueous Solution via Persulfate Activation, *Appl. Surf. Sci.*, 2016, **369**, 130–136, DOI: **10.1016/j.apsusc.2016.02.037**.

150 S. Marx, W. Kleist, J. Huang, M. Maciejewski and A. Baiker, Tuning Functional Sites and Thermal Stability of Mixed-Linker MOFs Based on MIL-53(Al), *Dalton Trans.*, 2010, **39**(16), 3795–3798, DOI: **10.1039/C002483J**.

151 A. Chatterjee, A. K. Jana and J. K. Basu, Silica Supported Binary Metal Organic Framework for Removing Organic Dye Involving Combined Effect of Adsorption Followed by Photocatalytic Degradation, *Mater. Res. Bull.*, 2021, **138**, 111227, DOI: **10.1016/j.materresbull.2021.111227**.

152 V. Russo, M. Hmoudah, F. Broccoli, M. R. Iesce, O.-S. Jung and M. Di Serio, Applications of Metal Organic Frameworks in Wastewater Treatment: A Review on Adsorption and Photodegradation, *Front. Chem. Eng.*, 2020, **2**, 581487.

153 T. Araya, M. Jia, J. Yang, P. Zhao, K. Cai, W. Ma and Y. Huang, Resin Modified MIL-53 (Fe) MOF for Improvement of Photocatalytic Performance, *Appl. Catal., B*, 2017, **203**, 768–777, DOI: **10.1016/j.apcatb.2016.10.072**.

154 H. Han and H. Frei, Controlled Assembly of Hetero-Binuclear Sites on Mesoporous Silica: Visible Light Charge-Transfer Units with Selectable Redox Properties, *J. Phys. Chem. C*, 2008, **112**(22), 8391–8399, DOI: **10.1021/jp800556g**.

155 H. Shahriyari Far, M. Najafi, M. Hasanzadeh and R. Rahimi, Synthesis of MXene/Metal–Organic Framework (MXOF) Composite as an Efficient Photocatalyst for Dye Contaminant Degradation, *Inorg. Chem. Commun.*, 2023, **152**, 110680, DOI: **10.1016/j.inoche.2023.110680**.

156 M. Arif, U. Fatima, A. Rauf, Z. H. Farooqi, M. Javed, M. Faizan and S. Zaman, A New 2D Metal–Organic Framework for Photocatalytic Degradation of Organic

Dyes in Water, *Catalysts*, 2023, **13**(2), 231, DOI: 10.3390/catal13020231.

157 M. Kim, J. S. Oh, B. H. Kim, A. Y. Kim, K. C. Park, J. Mun, G. Gupta and C. Y. Lee, Enhanced Photocatalytic Performance of Nanosized Mixed-Ligand Metal–Organic Frameworks through Sequential Energy and Electron Transfer Process, *Inorg. Chem.*, 2020, **59**(17), 12947–12953, DOI: 10.1021/acs.inorgchem.0c02079.

158 H. Li, Y. Yao, J. Zhang, J. Du, S. Xu, C. Wang, D. Zhang, J. Tang, H. Zhao and J. Zhou, Degradation of Phenanthrene by Peroxymonosulfate Activated with Bimetallic Metal–Organic Frameworks: Kinetics, Mechanisms, and Degradation Products, *Chem. Eng. J.*, 2020, **397**, 125401, DOI: 10.1016/j.cej.2020.125401.

159 M.-J. Tsai, M.-Y. Chung, M.-Y. Kuo and J.-Y. Wu, Effective Enhancement of Performances on Photo-Assisted Dye Degradation Using a Zn Coordination Polymer and Its Post-Modified Cu/Zn Bimetallic Analogue under Natural Environments, *J. Environ. Chem. Eng.*, 2023, **11**(2), 109258, DOI: 10.1016/j.jece.2022.109258.

160 K. Divyarani, S. Sreenivasa, T. M. C. Rao, W. Nabgan, F. A. Alharthi, B.-H. Jeon and L. Parashuram, Boosting Sulfate Radical Assisted Photocatalytic Advanced Oxidative Degradation of Tetracycline via Few-Layered CoZn@MOF/GO Nanosheets, *Colloids Surf., A*, 2023, **671**, 131606, DOI: 10.1016/j.colsurfa.2023.131606.

161 W. Wang, D. Wang, H. Song, D. Hao, B. Xu, J. Ren, M. Wang, C. Dai, Y. Wang and W. Liu, Size Effect of Gold Nanoparticles in Bimetallic ZIF Catalysts for Enhanced Photo-Redox Reactions, *Chem. Eng. J.*, 2023, **455**, 140909, DOI: 10.1016/j.cej.2022.140909.

162 S. Shi, P. Guo, M. I. Anwar, W. Zhang, W. Zhang and G. Yang, Copper Mixed-Triazolate Frameworks Featuring the Thiophene-Containing Ligand towards Enhanced Photodegradation of Organic Contaminants in Water, *J. Hazard. Mater.*, 2021, **406**, 124757, DOI: 10.1016/j.jhazmat.2020.124757.

163 J. Wang, S. Zhou, G. Wang, W. Hu, A. Kumar and M. Muddassir, Modular Construction and Photocatalytic Properties of Two Co(II) Metal–Organic Frameworks, *J. Mol. Struct.*, 2021, **1223**, 129218, DOI: 10.1016/j.molstruc.2020.129218.

164 N. Zhao, F. Sun, N. Zhang and G. Zhu, Novel pyrene-based anionic metal–organic framework for efficient organic dye elimination, *Cryst. Growth Des.*, 2017, **17**(5), 2453–2457, DOI: 10.1021/acs.cgd.6b01864.

165 K. Fan, W.-X. Nie, L.-P. Wang, C.-H. Liao, S.-S. Bao and L.-M. Zheng, Defective Metal–Organic Frameworks Incorporating Iridium-Based Metalloligands: Sorption and Dye Degradation Properties, *Chem.–Eur. J.*, 2017, **23**(27), 6615–6624, DOI: 10.1002/chem.201700365.

166 D. Guo, R. Wen, M. Liu, H. Guo, J. Chen and W. Weng, Facile Fabrication of G-C_3N_4/MIL-53(Al) Composite with Enhanced Photocatalytic Activities under Visible-Light Irradiation, *Appl. Organomet. Chem.*, 2015, **29**(10), 690–697, DOI: 10.1002/aoc.3352.

167 X. Liu, J. Zhang, Y. Dong, H. Li, Y. Xia and H. Wang, A Facile Approach for the Synthesis of Z-Scheme Photocatalyst ZIF-8/g-C_3N_4 with Highly Enhanced Photocatalytic Activity under Simulated Sunlight, *New J. Chem.*, 2018, **42**(14), 12180–12187, DOI: 10.1039/C8NJ01782D.

168 Y. Zhu, M. Zhu, H. Lv, S. Zhao, X. Shen, Q. Zhang, W. Zhu and B. Li, Coating BiOCl@g-C_3N_4 Nanocomposite with a Metal Organic Framework: Enhanced Visible Light Photocatalytic Activities, *J. Solid State Chem.*, 2020, **292**, 121641, DOI: 10.1016/j.jssc.2020.121641.

169 Y. Chen, B. Zhai, Y. Liang and Y. Li, Hybrid photocatalysts using semiconductor/MOF/graphene oxide for superior photodegradation of organic pollutants under visible light, *Mater. Sci. Semicond. Process.*, 2020, **107**, 104838, DOI: 10.1016/j.mssp.2019.104838.

170 J. Mao, M. Ge, J. Huang, Y. Lai, C. Lin, K. Zhang, K. Meng and Y. Tang, Constructing Multifunctional MOF@rGO Hydro-/Aerogels by the Self-Assembly Process for Customized Water Remediation, *J. Mater. Chem. A*, 2017, **5**(23), 11873–11881, DOI: 10.1039/C7TA01343D.

171 X.-H. Chen, Y.-S. Zhang, W.-B. Li, X.-W. Guan, J.-W. Ye, L. Chen, H.-P. Wang, J. Bai, Z.-W. Mo and X.-M. Chen, A Porphyrin-Based Metal–Organic Framework with Highly Efficient Adsorption and Photocatalytic Degradation Performances for Organic Dyes, *Inorg. Chem. Front.*, 2022, **9**(10), 2328–2335, DOI: 10.1039/D2QI00091A.

172 Z.-H. Zhu, Y. Liu, C. Song, Y. Hu, G. Feng and B. Z. Tang, Porphyrin-Based Two-Dimensional Layered Metal–Organic Framework with Sono-/Photocatalytic Activity for Water Decontamination, *ACS Nano*, 2022, **16**(1), 1346–1357, DOI: 10.1021/acsnano.1c09301.

173 Z. Shao, X. Han, Y. Liu, W. Xu, Q. Wu, Q. Xie, Y. Zhao and H. Hou, Metal-Dependent Photocatalytic Activity and Magnetic Behaviour of a Series of 3D Co–Ni Metal Organic Frameworks, *Dalton Trans.*, 2019, **48**(18), 6191–6197, DOI: 10.1039/C9DT00968J.

174 X. Wu, X. Shen, S. Fan, M. Trivedi, B. Li, A. Kumar and J. Liu, The Utilization of a Stable 2D Bilayer MOF for Simultaneous Study of Luminescent and Photocatalytic Properties: Experimental Studies and Theoretical Analysis, *RSC Adv.*, 2018, **8**(42), 23529–23538, DOI: 10.1039/C8RA04145H.

175 S.-H. Zhou, J. Wang, Y.-W. Liu, Y. Zhong, Y.-C. Sun, B. Xie, A. Ma, A. Singh, M. Muddassir and A. Kumar, Structures and Photocatalytic Properties of Two New Zn(II) Coordination Polymers Based on Semi-Rigid V-Shaped Multicarboxylate Ligands, *RSC Adv.*, 2020, **10**(32), 18721–18727, DOI: 10.1039/D0RA02222E.

176 S. Dai, Y. Liu, Y. Li, N. Jin, X. Wang, X. Liu, H. Chen, Y. Zhao, H. Luo and W. Li, Three Novel Coordination Polymers as Bifunctional Materials for the Photocatalytic Degradation of Dyes and the Oxygen Evolution Reaction in Alkaline Solutions, *CrystEngComm*, 2023, **25**(5), 785–797, DOI: 10.1039/D2CE01306A.

177 S. Ahmed, A. Kumar and P. Sarathi Mukherjee, A Benzothiadiazole-Based Pt(II) Coordination Polymer as an Efficient Heterogeneous Photocatalyst for Visible-Light-

Driven Aerobic Oxidative Coupling of Amines, *Chem. Commun.*, 2023, **59**(22), 3229–3232, DOI: **10.1039/D3CC00021D**.

178 N. M. Mahmoodi, J. Abdi, M. Oveisi, M. Alinia Asli and M. Vossoughi, Metal–Organic Framework (MIL-100 (Fe)): Synthesis, Detailed Photocatalytic Dye Degradation Ability in Colored Textile Wastewater and Recycling, *Mater. Res. Bull.*, 2018, **100**, 357–366, DOI: **10.1016/j.materresbull.2017.12.033**.

179 H. Li, J. Zhang, Y. Yao, X. Miao, J. Chen and J. Tang, Nanoporous Bimetallic Metal–Organic Framework (FeCo-BDC) as a Novel Catalyst for Efficient Removal of Organic Contaminants, *Environ. Pollut.*, 2019, **255**, 113337, DOI: **10.1016/j.envpol.2019.113337**.

180 *Pd Nanoparticles Supported on MIL-101/Reduced Graphene Oxide Photocatalyst: An Efficient and Recyclable Photocatalyst for Triphenylmethane Dye Degradation | SpringerLink*, **https://link.springer.com/article/10.1007/s11356-015-5364-z**, (accessed 2023-05-16).

181 L. Xia, J. Ni, P. Wu, J. Ma, L. Bao, Y. Shi and J. Wang, Photoactive Metal–Organic Framework as a Bifunctional Material for 4-Hydroxy-4′-Nitrobiphenyl Detection and Photodegradation of Methylene Blue, *Dalton Trans.*, 2018, **47**(46), 16551–16557, DOI: **10.1039/C8DT03278E**.

182 *Highly Efficient Photocatalytic Degradation of Dyes by a Copper–Triazolate Metal–Organic Framework – Liu – 2018 – Chemistry – A European Journal – Wiley Online Library*, **https://chemistry-europe.onlinelibrary.wiley.com/doi/abs/10.1002/chem.201803306**, (accessed 2023-05-16).

183 *Construction of Mixed-Valence Cu(I)/Cu(II) 3-D Framework and Its Photocatalytic Activities – ScienceDirect*, **https://www.sciencedirect.com/science/article/pii/S0277538718303292**, (accessed 2023-05-16).

184 H. Li, Q. Li, X. He, Z. Xu, Y. Wang and L. Jia, Synthesis of AgBr@MOFs Nanocomposite and Its Photocatalytic Activity for Dye Degradation, *Polyhedron*, 2019, **165**, 31–37, DOI: **10.1016/j.poly.2019.02.050**.

185 J.-J. Du, Y.-P. Yuan, J.-X. Sun, F.-M. Peng, X. Jiang, L.-G. Qiu, A.-J. Xie, Y.-H. Shen and J.-F. Zhu, New Photocatalysts Based on MIL-53 Metal–Organic Frameworks for the Decolorization of Methylene Blue Dye, *J. Hazard. Mater.*, 2011, **190**(1), 945–951, DOI: **10.1016/j.jhazmat.2011.04.029**.

186 *TiO_2 Nanoparticles Anchored onto the Metal–Organic Framework NH_2-MIL-88B(Fe) as an Adsorptive Photocatalyst with Enhanced Fenton-like Degradation of Organic Pollutants under Visible Light Irradiation | ACS Sustainable Chemistry & Engineering*, **https://pubs.acs.org/doi/full/10.1021/acssuschemeng.8b02968**, (accessed 2023-05-16).

187 S. Gholizadeh Khasevani and M. R. Gholami, Evaluation of the Reaction Mechanism for Photocatalytic Degradation of Organic Pollutants with MIL-88A/BiOI Structure under Visible Light Irradiation, *Res. Chem. Intermed.*, 2019, **45**(3), 1341–1356, DOI: **10.1007/s11164-018-3681-9**.

188 *Synthesis of BiOI/$ZnFe_2O_4$–Metal–Organic Framework and g-C_3N_4-Based Nanocomposites for Applications in Photocatalysis | Industrial & Engineering Chemistry Research*, **https://pubs.acs.org/doi/full/10.1021/acs.iecr.8b05871**, (accessed 2023-05-16).

189 X. Li, Y. Pi, L. Wu, Q. Xia, J. Wu, Z. Li and J. Xiao, Facilitation of the Visible Light-Induced Fenton-like Excitation of H_2O_2 via Heterojunction of g-C_3N_4/NH_2-Iron Terephthalate Metal–Organic Framework for MB Degradation, *Appl. Catal., B*, 2017, **202**, 653–663, DOI: **10.1016/j.apcatb.2016.09.073**.

190 X. Liu, R. Dang, W. Dong, X. Huang, J. Tang, H. Gao and G. Wang, A Sandwich-like Heterostructure of TiO_2 Nanosheets with MIL-100(Fe): A Platform for Efficient Visible-Light-Driven Photocatalysis, *Appl. Catal., B*, 2017, **209**, 506–513, DOI: **10.1016/j.apcatb.2017.02.073**.

191 F. Martínez, P. Leo, G. Orcajo, M. Díaz-García, M. Sanchez-Sanchez and G. Calleja, Sustainable Fe-BTC Catalyst for Efficient Removal of Mehylene Blue by Advanced Fenton Oxidation, *Catal. Today*, 2018, **313**, 6–11, DOI: **10.1016/j.cattod.2017.10.002**.

192 H. Lv, H. Zhao, T. Cao, L. Qian, Y. Wang and G. Zhao, Efficient Degradation of High Concentration Azo-Dye Wastewater by Heterogeneous Fenton Process with Iron-Based Metal–Organic Framework, *J. Mol. Catal. A: Chem.*, 2015, **400**, 81–89, DOI: **10.1016/j.molcata.2015.02.007**.

193 Y. Liu, Y. Xie, M. Dai, Q. Gong and Z. Dang, Ag/AgCl/MIL-101(Fe) Catalyzed Degradation of Methylene Blue under Visible Light Irradiation, *Materials*, 2019, **12**(9), 1453, DOI: **10.3390/ma12091453**.

194 Q. Liang, M. Zhang, Z. Zhang, C. Liu, S. Xu and Z. Li, Zinc Phthalocyanine Coupled with UIO-66 (NH_2) via a Facile Condensation Process for Enhanced Visible-Light-Driven Photocatalysis, *J. Alloys Compd.*, 2017, **690**, 123–130, DOI: **10.1016/j.jallcom.2016.08.087**.

195 R. Zhang, B. Du, Q. Li, Z. Cao, G. Feng and X. Wang, α-Fe_2O_3 Nanoclusters Confined into UiO-66 for Efficient Visible-Light Photodegradation Performance, *Appl. Surf. Sci.*, 2019, **466**, 956–963, DOI: **10.1016/j.apsusc.2018.10.048**.

196 H.-P. Jing, C.-C. Wang, Y.-W. Zhang, P. Wang and R. Li, Photocatalytic Degradation of Methylene Blue in ZIF-8, *RSC Adv.*, 2014, **4**(97), 54454–54462, DOI: **10.1039/C4RA08820D**.

197 J. Zhang, S. Bhattacharya, A. B. Müller, L. Kiss, C. Silvestru, N. Kuhnert and U. Kortz, Mixed Noble Metal–Oxo Clusters: Platinum(IV)–Gold(III)Oxoanion[$PtIV_2AuIII_3O_6((CH_3)_2AsO_2)_6$], *Chem. Commun.*, 2023, **59**(39), 5918–5921, DOI: **10.1039/D3CC00243H**.

198 *Space-Confined Nucleation of Semimetal-Oxo Clusters within a [H7P8W48O184]33 – Macrocycle: Synthesis, Structure, and Enhanced Proton Conductivity | Inorganic Chemistry*, **https://pubs.acs.org/doi/full/10.1021/acs.inorgchem.2c03543** , (accessed 2023-05-21).

199 R. Sen Gupta, S. Mandal, S. Arya, S. Dutta, K. Manna, Sk. Safikul Islam, S. Pathan and S. Bose, Copper-Substituted Polyoxometalate-Soldered Interpenetrating Polymeric Networks Membranes for Water Remediation, *Chem. Eng. J.*, 2023, **461**, 141949, DOI: **10.1016/j.cej.2023.141949**.

200 R. Rajak, M. Saraf, A. Mohammad and S. M. Mobin, Design and Construction of a Ferrocene Based Inclined Polycatenated Co-MOF for Supercapacitor and Dye Adsorption Applications, *J. Mater. Chem. A*, 2017, **5**(34), 17998–18011, DOI: **10.1039/C7TA03773B**.

201 F. Fan, S. Feng, L. Zhao, L. Zhang, X. Zhang, T. Wang and Y. Fu, Preparation of Redox-Active Metal–Organic Frameworks via Post-Synthetic Modification of Organic Selenium for In Situ Confinement of Metal Nanoparticles, *Adv. Mater. Interfaces*, 2022, **9**(25), 2200995, DOI: **10.1002/admi.202200995**.

202 M. Singh, A. Karmakar, N. Seal, P. P. Mondal, S. Kundu and S. Neogi, Redox-Active and Urea-Engineered-Entangled MOFs for High-Efficiency Water Oxidation and Elevated Temperature Advanced CO_2 Separation Cum Organic-Site-Driven Mild-Condition Cycloaddition, *ACS Appl. Mater. Interfaces*, 2023, **15**(20), 24504–24516, DOI: **10.1021/acsami.3c03619**.

203 Z. Ma, B. Guan, J. Guo, X. Wu, Y. Chen, J. Zhang, X. Jiang, S. Bao, L. Chen, K. Shu, H. Dang, Z. Guo, Z. Li, S. Yao and Z. Huang, State of the Art and Prospectives of Heterogeneous Photocatalysts Based on Metal–Organic Frameworks (MOFs): Design, Modification Strategies, and Their Applications and Mechanisms in Photodegradation, Water Splitting, and CO_2 Reduction, *Catal. Sci. Technol.*, 2023, **13**(15), 4285–4347, DOI: **10.1039/D3CY00479A**.

204 J. Lan, Y. Wang, B. Huang, Z. Xiao and P. Wu, Application of Polyoxometalates in Photocatalytic Degradation of Organic Pollutants, *Nanoscale Adv.*, 2021, **3**(16), 4646–4658, DOI: **10.1039/D1NA00408E**.

205 *Structural and Magnetical Studies of Mixed-Valence Hexavanadate Hybrids: How Organic Ligands Affect the Magnetism of Polyoxometalates?* | *Inorganic Chemistry*, **https://pubs.acs.org/doi/10.1021/acs.inorgchem.1c00044**, (accessed 2023-05-29).

206 M. Wang, G. Tan, M. Dang, Y. Wang, B. Zhang, H. Ren, L. Lv and A. Xia, Dual Defects and Build-in Electric Field Mediated Direct Z-Scheme W18O49/g-C_3N_{4-x} Heterojunction for Photocatalytic NO Removal and Organic Pollutant Degradation, *J. Colloid Interface Sci.*, 2021, **582**, 212–226, DOI: **10.1016/j.jcis.2020.08.040**.

207 R. Liu and C. Streb, Polyoxometalate-Single Atom Catalysts (POM-SACs) in Energy Research and Catalysis, *Adv. Energy Mater.*, 2021, **11**(25), 2101120, DOI: **10.1002/aenm.202101120**.

208 R. Wang, Y. Feng, L. Jiao, Y. Dong, H. Zhou, T. Liu, X. Jing and H. Lv, Size-Matching Encapsulation of a High-Nuclearity Ni-Containing Polyoxometalate into a Light-Responsive MOF for Robust Photogeneration of Hydrogen, *J. Mater. Chem. A*, 2023, **11**(11), 5811–5818, DOI: **10.1039/D2TA09606D**.

209 S. Zhang, F. Ou, S. Ning and P. Cheng, Polyoxometalate-Based Metal–Organic Frameworks for Heterogeneous Catalysis, *Inorg. Chem. Front.*, 2021, **8**(7), 1865–1899, DOI: **10.1039/D0QI01407A**.

210 X. Song, D. Hu, X. Yang, H. Zhang, W. Zhang, J. Li, M. Jia and J. Yu, Polyoxomolybdic Cobalt Encapsulated within Zr-Based Metal–Organic Frameworks as Efficient Heterogeneous Catalysts for Olefins Epoxidation, *ACS Sustain. Chem. Eng.*, 2019, **7**(3), 3624–3631, DOI: **10.1021/acssuschemeng.8b06736**.

211 S. Wang, Y. Liu, Z. Zhang, X. Li, H. Tian, T. Yan, X. Zhang, S. Liu, X. Sun, L. Xu, F. Luo and S. Liu, One-Step Template-Free Fabrication of Ultrathin Mixed-Valence Polyoxovanadate-Incorporated Metal–Organic Framework Nanosheets for Highly Efficient Selective Oxidation Catalysis in Air, *ACS Appl. Mater. Interfaces*, 2019, **11**(13), 12786–12796, DOI: **10.1021/acsami.9b00908**.

212 Q. Huang, J. Liu, L. Feng, Q. Wang, W. Guan, L.-Z. Dong, L. Zhang, L.-K. Yan, Y.-Q. Lan and H.-C. Zhou, Multielectron Transportation of Polyoxometalate-Grafted Metalloporphyrin Coordination Frameworks for Selective CO_2-to-CH_4 Photoconversion, *Natl. Sci. Rev.*, 2020, **7**(1), 53–63, DOI: **10.1093/nsr/nwz096**.

213 H. N. Miras, L. Vilà-Nadal and L. Cronin, Polyoxometalate Based Open-Frameworks (POM-OFs), *Chem. Soc. Rev.*, 2014, **43**(16), 5679–5699, DOI: **10.1039/C4CS00097H**.

214 D.-G. Ke, S.-L. Huang and G.-Y. Yang, Lanthanide-Anderson Polyoxometalates Frameworks: Efficient Sulfide Photooxidation, *Inorg. Chem.*, 2022, **61**(49), 20080–20086, DOI: **10.1021/acs.inorgchem.2c03504**.

215 S.-B. Yu, F. Lin, J. Tian, J. Yu, D.-W. Zhang and Z.-T. Li, Water-Soluble and Dispersible Porous Organic Polymers: Preparation, Functions and Applications, *Chem. Soc. Rev.*, 2022, **51**(2), 434–449, DOI: **10.1039/D1CS00862E**.

216 X. Chen, H. Wu, X. Shi and L. Wu, Polyoxometalate-Based Frameworks for Photocatalysis and Photothermal Catalysis, *Nanoscale*, 2023, **15**, 9242–9255, DOI: **10.1039/D3NR01176C**.

217 Y. Cui, Y. Zhao, J. Wu and H. Hou, Recent Discussions on Homogeneous Host–Guest Metal–Organic Framework Composites in Synthesis and Catalysis, *Nano Today*, 2023, **52**, 101972, DOI: **10.1016/j.nantod.2023.101972**.

218 X. Liu, B. Qian, D. Zhang, M. Yu, Z. Chang and X. Bu, Recent Progress in Host–Guest Metal–Organic Frameworks: Construction and Emergent Properties, *Coord. Chem. Rev.*, 2023, **476**, 214921, DOI: **10.1016/j.ccr.2022.214921**.

219 Y. Hu, J. Liu, C. Lee, M. Li, B. Han, T. Wu, H. Pan, D. Geng and Q. Yan, Integration of Metal–Organic Frameworks and Metals: Synergy for Electrocatalysis, *Small*, 2023, **19**(32), 2300916, DOI: **10.1002/smll.202300916**.

220 J. Shi, Z. Su, X. Li, J. Feng and C. Men, Impacts of Host–Guest Assembly on the Photophysical and Photocatalytic Properties of Heterogenized Molecular Photosensitizer and Catalysts, *J. Mater. Chem. A*, 2023, **11**(13), 6646–6658, DOI: **10.1039/D2TA09715J**.

221 *Synthesis and Structures of a New Series of Silver-Vanadate Hybrid Solids and Their Optical and Photocatalytic Properties* | *Inorganic Chemistry*, **https://pubs.acs.org/doi/full/10.1021/ic8004129**, (accessed 2023-05-16).

222 *Lanthanide–Organic Cation Frameworks with Zeolite Gismondine Topology and Large Cavities from Intersected Channels Templated by Polyoxometalate Counterions* |

Inorganic Chemistry, https://pubs.acs.org/doi/full/10.1021/ic801846h, (accessed 2023-05-16).

223 B. Liu, J. Yang, G. C. Yang and J. F. Ma, Four new three-dimensional polyoxometalate-based metal–organic frameworks constructed from $[Mo_6O_{18}(O_3AsPh)_2]_4^-$ polyoxoanions and copper(I)-organic fragments: syntheses, structures, electrochemistry, and photocatalysis properties, *Inorg. Chem.*, 2013, **52**(1), 84–94, DOI: 10.1021/ic301257k.

224 H. Yang, T. Liu, M. Cao, H. Li, S. Gao and R. Cao, A Water-Insoluble and Visible Light Induced Polyoxometalate-Based Photocatalyst, *Chem. Commun.*, 2010, **46**(14), 2429–2431, DOI: 10.1039/B919868G.

225 C. M. Granadeiro, D. Julião, S. O. Ribeiro, L. Cunha-Silva and S. S. Balula, Recent Advances in Lanthanide-Coordinated Polyoxometalates: From Structural Overview to Functional Materials, *Coord. Chem. Rev.*, 2023, **476**, 214914, DOI: 10.1016/j.ccr.2022.214914.

226 *Structural and Photocatalytic Activity of Lanthanide (Ce, Pr, and Nd) Molybdovanadates | The Journal of Physical Chemistry C*, https://pubs.acs.org/doi/full/10.1021/jp069007e, (accessed 2023-05-16).

227 X. Chen, Y. Chen, Z. Xia, H. Hu, Y. Sun and W. S. Huang, Crystal Structure of α-Keggin Heteropolymolybdates with Pyridine-2,6-Dicarboxylate Based Frameworks, and Associated RhB Photocatalytic Degradation and 2D-IR COS Tests, *Dalton Trans.*, 2012, **41**(33), 10035–10042, DOI: 10.1039/C2DT00001F.

228 J. Xu, Y. Ao, D. Fu and C. Yuan, Study on Photocatalytic Performance and Degradation Kinetics of X-3B with Lanthanide-Modified Titanium Dioxide under Solar and UV Illumination, *J. Hazard. Mater.*, 2009, **164**(2), 762–768, DOI: 10.1016/j.jhazmat.2008.08.108.

229 K. Wang, D. Zhang, J. Ma, P. Ma, J. Niu and J. Wang, Three-Dimensional Lanthanide Polyoxometalate Organic Complexes: Correlation of Structure with Properties, *CrystEngComm*, 2012, **14**(9), 3205–3212, DOI: 10.1039/C2CE06492H.

230 W. Zhu, X.-Y. Yang, Y.-H. Li, J.-P. Li, D. Wu, Y. Gao and F.-Y. Yi, A Novel Porous Molybdophosphate-Based FeII,III-MOF Showing Selective Dye Degradation as a Recyclable Photocatalyst, *Inorg. Chem. Commun.*, 2014, **49**, 159–162, DOI: 10.1016/j.inoche.2014.09.033.

231 *Co-Immobilization of a Rh Catalyst and a Keggin Polyoxometalate in the UiO-67 Zr-Based Metal–Organic Framework: In Depth Structural Characterization and Photocatalytic Properties for CO_2 Reduction | Journal of the American Chemical Society*, https://pubs.acs.org/doi/full/10.1021/jacs.0c02425, (accessed 2023-05-16).

232 D.-M. Chen, X.-H. Liu, N.-N. Zhang, C.-S. Liu and M. Du, Immobilization of Polyoxometalate in a Cage-Based Metal–Organic Framework towards Enhanced Stability and Highly Effective Dye Degradation, *Polyhedron*, 2018, **152**, 108–113, DOI: 10.1016/j.poly.2018.05.059.

233 D.-M. Chen and X.-J. Zhang, A Polyoxometalate Template Metal–Organic Framework with Unusual $\{Cu_8(M_4\text{-}OH)_6\}_{10}$+ Secondary Building Unit for Photocatalytic Dye Degradation, *Inorg. Chem. Commun.*, 2019, **108**, 107523, DOI: 10.1016/j.inoche.2019.107523.

234 M. Ali, E. Pervaiz, T. Noor, O. Rabi, R. Zahra and M. Yang, Recent Advancements in MOF-Based Catalysts for Applications in Electrochemical and Photoelectrochemical Water Splitting: A Review, *Int. J. Energy Res.*, 2021, **45**(2), 1190–1226, DOI: 10.1002/er.5807.

235 S. Tasleem, M. Tahir and W. A. Khalifa, Current Trends in Structural Development and Modification Strategies for Metal–Organic Frameworks (MOFs) towards Photocatalytic H_2 Production: A Review, *Int. J. Hydrogen Energy*, 2021, **46**(27), 14148–14189, DOI: 10.1016/j.ijhydene.2021.01.162.

236 *Rational Design of Metal–Organic Framework-Based Materials for Photocatalytic CO_2 Reduction – Zhan – 2022 – Advanced Energy and Sustainability Research – Wiley Online Library*, https://onlinelibrary.wiley.com/doi/full/10.1002/aesr.202200004, (accessed 2023-05-16).

237 *Density Functional Theory of Electronic Structure | The Journal of Physical Chemistry*, https://pubs.acs.org/doi/full/10.1021/jp960669l, (accessed 2023-05-16).

238 *Perspective: Kohn–Sham Density Functional Theory Descending a Staircase | The Journal of Chemical Physics | AIP Publishing*, https://pubs.aip.org/aip/jcp/article/145/13/130901/280869/Perspective-Kohn-Sham-density-functional-theory, (accessed 2023-05-16).

239 C. Adamo and D. Jacquemin, The Calculations of Excited-State Properties with Time-Dependent Density Functional Theory, *Chem. Soc. Rev.*, 2013, **42**(3), 845–856, DOI: 10.1039/C2CS35394F.

240 J. P. Perdew, K. Burke and M. Ernzerhof, Generalized Gradient Approximation Made Simple, *Phys. Rev. Lett.*, 1996, **77**(18), 3865–3868, DOI: 10.1103/PhysRevLett.77.3865.

241 I. Choudhuri and D. G. Truhlar, HLE17: An Efficient Way To Predict Band Gaps of Complex Materials, *J. Phys. Chem. C*, 2019, **123**(28), 17416–17424, DOI: 10.1021/acs.jpcc.9b04683.

242 S. Huang, Z. Wang, Y. Von Lim, Y. Wang, Y. Li, D. Zhang and H. Y. Yang, Recent Advances in Heterostructure Engineering for Lithium–Sulfur Batteries, *Adv. Energy Mater.*, 2021, **11**(10), 2003689, DOI: 10.1002/aenm.202003689.

243 D. Kong, Y. Wang, Y. Wang, S. Huang, J. Hu, J. Hu, Y. Von Lim, B. Liu, B. Liu, B. Liu, B. Liu, S. Fan, Y. Shi and H. Y. Yang, 3D Self-Branched Zinc–Cobalt Oxide@N-Doped Carbon Hollow Nanowall Arrays for High-Performance Asymmetric Supercapacitors and Oxygen Electrocatalysis, *Energy Storage Mater.*, 2019, **23**, 653–663, DOI: 10.1016/j.ensm.2019.03.003.

244 S. Huang, Y. V. Lim, X. Zhang, Y. Wang, Y. Zheng, D. Kong, M. Ding, S. A. Yang and H. Y. Yang, Regulating the Polysulfide Redox Conversion by Iron Phosphide Nanocrystals for High-Rate and Ultrastable Lithium–Sulfur Battery, *Nano Energy*, 2018, **51**, 340–348, DOI: 10.1016/j.nanoen.2018.06.052.

245 Y. He, E. D. Cubuk, M. D. Allendorf and E. J. Reed, Metallic Metal–Organic Frameworks Predicted by the Combination of Machine Learning Methods and Ab Initio Calculations, *J. Phys. Chem. Lett.*, 2018, **9**(16), 4562–4569, DOI: **10.1021/acs.jpclett.8b01707**.

246 H. Xiao, J. Tahir-Kheli and W. A. I. Goddard, Accurate Band Gaps for Semiconductors from Density Functional Theory, *J. Phys. Chem. Lett.*, 2011, **2**(3), 212–217, DOI: **10.1021/jz101565j**.

247 A. L. Linsebigler, G. Lu and J. T. Yates Jr., Photocatalysis on TiO_2 Surfaces: Principles, Mechanisms, and Selected Results, *Chem. Rev.*, 1995, **95**(3), 735–758, DOI: **10.1021/cr00035a013**.

248 *Computational Design of Functionalized Metal–Organic Framework Nodes for Catalysis | ACS Central Science*, **https://pubs.acs.org/doi/full/10.1021/acscentsci.7b00500**, (accessed 2023-05-16).

249 H. Li, M. Eddaoudi, M. O'Keeffe and O. M. Yaghi, Design and Synthesis of an Exceptionally Stable and Highly Porous Metal–Organic Framework, *Nature*, 1999, **402**(6759), 276–279, DOI: **10.1038/46248**.

250 M. Fuentes-Cabrera, D. M. Nicholson, B. G. Sumpter and M. Widom, Electronic Structure and Properties of Isoreticular Metal–Organic Frameworks: The Case of M-IRMOF1 (M = Zn, Cd, Be, Mg, and Ca), *J. Chem. Phys.*, 2005, **123**(12), 124713, DOI: **10.1063/1.2037587**.

251 L.-M. Yang, P. Vajeeston, P. Ravindran, H. Fjellvåg and M. Tilset, Theoretical Investigations on the Chemical Bonding, Electronic Structure, And Optical Properties of the Metal–Organic Framework MOF-5, *Inorg. Chem.*, 2010, **49**(22), 10283–10290, DOI: **10.1021/ic100694w**.

252 L.-M. Yang, P. Vajeeston, P. Ravindran, H. Fjellvåg and M. Tilset, Revisiting Isoreticular MOFs of Alkaline Earth Metals : A Comprehensive Study on Phase Stability, Electronic Structure, Chemical Bonding, and Optical Properties of A–IRMOF-1 (A = Be, Mg, Ca, Sr, Ba), *Phys. Chem. Chem. Phys.*, 2011, **13**(21), 10191–10203, DOI: **10.1039/C0CP02944K**.

253 *Band Gap Engineering of Paradigm MOF-5 | Crystal Growth & Design*, **https://pubs.acs.org/doi/full/10.1021/cg500243s**, (accessed 2023-05-16).

254 A. Kuc, A. Enyashin and G. Seifert, Metal–Organic Frameworks: Structural, Energetic, Electronic, and Mechanical Properties, *J. Phys. Chem. B*, 2007, **111**(28), 8179–8186, DOI: **10.1021/jp072085x**.

255 L. Valenzano, B. Civalleri, S. Chavan, S. Bordiga, M. H. Nilsen, S. Jakobsen, K. P. Lillerud and C. Lamberti, Disclosing the Complex Structure of UiO-66 Metal Organic Framework: A Synergic Combination of Experiment and Theory, *Chem. Mater.*, 2011, **23**(7), 1700–1718, DOI: **10.1021/cm1022882**.

256 L.-M. Yang, E. Ganz, S. Svelle and M. Tilset, Computational Exploration of Newly Synthesized Zirconium Metal–Organic Frameworks UiO-66, -67, -68 and Analogues, *J. Mater. Chem. C*, 2014, **2**(34), 7111–7125, DOI: **10.1039/C4TC00902A**.

257 A. Walsh and C. R. A. Catlow, Photostimulated Reduction Processes in a Titania Hybrid Metal–Organic Framework, *ChemPhysChem*, 2010, **11**(11), 2341–2344, DOI: **10.1002/cphc.201000306**.

258 C. H. Hendon, D. Tiana, M. Fontecave, C. Sanchez, L. D'arras, C. Sassoye, L. Rozes, C. Mellot-Draznieks and A. Walsh, Engineering the Optical Response of the Titanium-MIL-125 Metal–Organic Framework through Ligand Functionalization, *J. Am. Chem. Soc.*, 2013, **135**(30), 10942–10945, DOI: **10.1021/ja405350u**.

259 H. Li, X. Yang, L. You, H. Wang, P. Hu, W. Zhang, Z. Wang and X. Xie, Improving Detection Efficiency of Superconducting Nanowire Single-Photon Detector Using Multilayer Antireflection Coating, *AIP Adv.*, 2018, **8**(11), 115022, DOI: **10.1063/1.5034374**.

260 Z. Jiao, J. Zheng, C. Feng, Z. Wang, X. Wang, G. Lu and Y. Bi, Fe/W Co-Doped $BiVO_4$ Photoanodes with a Metal–Organic Framework Cocatalyst for Improved Photoelectrochemical Stability and Activity, *ChemSusChem*, 2016, **9**(19), 2824–2831, DOI: **10.1002/cssc.201600761**.

261 K. Hendrickx, D. E. P. Vanpoucke, K. Leus, K. Lejaeghere, A. Van Yperen-De Deyne, V. Van Speybroeck, P. Van Der Voort and K. Hemelsoet, Understanding Intrinsic Light Absorption Properties of UiO-66 Frameworks: A Combined Theoretical and Experimental Study, *Inorg. Chem.*, 2015, **54**(22), 10701–10710, DOI: **10.1021/acs.inorgchem.5b01593**.

262 K. Hendrickx, J. J. Joos, A. De Vos, D. Poelman, P. F. Smet, V. Van Speybroeck, P. Van Der Voort and K. Lejaeghere, Exploring Lanthanide Doping in UiO-66: A Combined Experimental and Computational Study of the Electronic Structure, *Inorg. Chem.*, 2018, **57**(9), 5463–5474, DOI: **10.1021/acs.inorgchem.8b00425**.

263 X.-P. Wu, L. Gagliardi and D. G. Truhlar, Cerium Metal–Organic Framework for Photocatalysis, *J. Am. Chem. Soc.*, 2018, **140**(25), 7904–7912, DOI: **10.1021/jacs.8b03613**.